Advances in Environmental Technology 4 (2021) 231-262

Advances in Environmental Technology

Iranian Research Organization for Science and Technology (IROST)

Journal home page: https://aet.irost.ir/

Using spatial statistics to identify drought-prone regions (A case study of Khuzestan Province, Iran)

Mohsen Nejadrekabi[1], Saeid Eslamian[1*2], Mohammad Javad Zareian[3]

[1]*Department of Civil Engineering, Najafabad Branch, Islamic Azad University, Najafabad, Iran*

[2]*Department of Water Engineering, College of Agriculture, Isfahan University of Technology, Isfahan, Iran*

[3]*Department of Water Resources Research, Water Research Institute (WRI), Tehran, Iran*

ARTICLE INFO

Article history:
Received 17 August 2021
Received in revised form
2 January 2022
Accepted 2 January 2022

Keywords:
Spatial statistics
Geostatistics
Spatial correlation
Anselin Local Moran index
Hot spots and cold spots

ABSTRACT

Iran is located in the Earth's arid zone, and a drought crisis imperils the country as a result of declining water resources. Khuzestan Province, located in the south of Iran, is in critical condition due to water shortages; many of its groves have been destroyed. It also has many respiratory and pulmonary patients due to the constant presence of dust. The pandemic and this dust have caused acute problems for those diagnosed with COVID-19. Due to the importance of water deficit in this province, the present research calculated the Standardized Precipitation Index (SPI) and Standard Precipitation Evaporation Index (SPEI) in a thirty-year statistical period from 1984 to 2014; 12 stations were selected during the months when rainfall was more likely. This study utilized a geostatistical method to prepare zoning maps of SPI and SPEI. Then, various spatial statistics techniques in ArcGIS software were used to identify and locate the exact areas that were the sources of drought with the help of drought hot spots and strong drought clusters. Anselin Local Moran's maps indicated that the high-high precipitation clusters were located in the northeastern regions of Khuzestan. The hot and cold drought spots, which were identified by Getis-Ord G* spatial statistics based on both SPI and SPEI, showed that the hot spots were formed in the southern and southwestern regions; the cold spots were formed in the northwestern regions. Furthermore, the drought hot spots were identified with a 99% confidence level in places where the total ten-year precipitation was less than 270 millimeters.

1. Introduction

Drought is an environmental phenomenon with a greater impact on arid and semi-arid regions of the world [1]. The actual trends of both meteorological and hydrological long-term changes appear to indicate that drought and water scarcity are likely to occur in the future due to climate change [2]. Iran's location in the dry belt and the reduction of water resources have turned the issue of drought into a serious crisis for the country. The mean

*Corresponding author: : +98 311 33913432
E-mail: saeid@cc.iut.ac.ir
DOI: 10.22104/AET.2021.5143.1397

precipitation in Iran is far behind the global average [3]. However, effective and well-timed drought monitoring can help develop drought forecasting systems, which can minimize the costs of drought. Drought indices are considered the primary tools for drought monitoring [4]. None of the provided indices for determining droughts can be utilized as a monitoring tool on its own. Several indices must be used simultaneously to increase the accuracy of drought monitoring. Different drought indices exist for providing desirable estimates regarding a drought's intensity, severity, and spatial extent. Various studies have focused on investigating influential factors on drought and developing drought indices to forecast this phenomenon. For instance, Vicente-Serrano *et al.* (2011) investigated the impacts of the warming process on droughts and water resources in Spain. They used SPI and SPEI, and concluded that both indices yield the same results [5]. Huang *et al.* (2014) [6] evaluated the spatiotemporal deviations of drought occurrence in Mongolia (North China) during 1960-2012. They used the SPI and three DS indices, including the number of dry spells (NDS), mean length of dry spells (MDS) and maximum length of dry spells (MxDS), and four periods (spring, summer, autumn, and winter). In another study, Rejaur Rahman and Habibah Lateh (2016) [7] analyzed meteorological droughts in Bangladesh using SPI, geographic information system (GIS), and monthly precipitation statistics by preparing the risk mapping. Besides, Ji Yae Shin *et al.* (2018) [8] investigated the propagation of meteorological droughts (using SPI) through the hydrological system using the Palmer hydrological drought index in South Korea. Modarres R. *et al.* (2007) [9] analyzed the annual rainfall time series, the annual number of rainy days, and the monthly rainfall of 20 stations to assess climate change in arid and semi-arid regions of Iran. Masroor, M. *et al.* (2021) [10] used specific spatial factors to determine the spots with groundwater potential. They utilized the Analytic Hierarchy Process (AHP) to determine the weight of factors and prepare the map of groundwater potential zones. They specified one-month droughts (meteorological), three- and six-month droughts (agricultural), and twelve-month droughts (hydrological) using the SPI during 1979-2013. Masroor *et al.* (2020) [11] assessed the drought conditions in the Godavari Middle Sub-basin of India using forty grid points data from global weather data for the SWAT portal during 1979–2013. They determined the SPI for one-month, three-month, six-month, and twelve-month drought and used the Mann-Kendall test and Sen's slope estimator to analyze the rainfall trend. Dariane (2003) [12] used the discrete ratio optimization model to control the performance of the reservoir dam during the drought period, which is done step by step. It indicated that for the number of similar second phase ration periods, the modified model's results were more favorable in reducing the damage caused by drought compared to the preliminary model. Harisuseno (2020) [13] revealed that the SPI method showed a moderately high correlation for all coefficients of correlation opposing to the PN method, which confirmed that the SPI method was more appropriate and reliable to assess drought characteristics. Ayad Ali Faris Beg *et al.* (2019) [14] calculated the mean SPI values and SPI frequencies for moist and dry conditions by applying GIS techniques based on long-term monthly precipitation data in Iraq from 1980 to 2010. The data were obtained using SPI software developed by the National Drought Mitigation Center, University of Nebraska-Lincoln. Likewise, Claudia Fernanda Almeida Teixeira-Gandra *et al.* (2019) [15] researched drought behavior identification. They used two meteorological indices, Standardized Precipitation Index (SPI) and Moreno Index (MI), specified for the state of Rio Grande do Sul, Brazil. Babaie Fini (2013) investigated the spatial analysis of long-term droughts in Iran by employing SPI and geostatistical methods and drew drought zoning maps in the GIS environment [16]. Hakimdoost *et al.* (2014) [17] investigated the spatial analysis of climate drought and its impact on the spatial location pattern of rural areas in Mazandaran villages. Furthermore, Jamalizadeh (2015) [18] analyzed droughts in Khuzestan Province over 20 years (1986-2005) by applying the SPI for short (3-6 months) and long (12, 24, and 48 months) periods using GIS software and the Inverse Distance Weighting (IDW) interpolation method. Regarding the process of destruction of Shadegan Ponds in Khuzestan Province, Mohammadi (2016) [19] points out: "for the past two decades, this pond has faced desolation as a consequence of excessive dam construction, drought, and insufficient attention". Afshar *et al.* (2021) [20] calculated meteorological droughts using SPI in more than 24000 pixels with a spatial resolution of 0.25 × 0.25 in Central Europe. They compared the heterogeneous mean values of VIs in dry and wet periods resulting from meteorological droughts statistically to evaluate the ability of VIs in drought conditions. Fei Xie and Hui Fan (2021) [21] examined the possibility of deriving drought indices from the MODIS VIs (EVI/NDVI) and the LST indices. They investigated three widely used reconstruction methods: the Savitzky-Golay filter, the Harmonic Analysis of Time Series Algorithm, and Whittaker smoother, in the Lancang-Mekong River Basin using MOD13Q1 and MOD11A2 products of the MODIS sensor and the Google Earth Engine cloud-based platform for the years 2001-2018. Agossou Gadedjisso-Tossou et al. (2021) [22] analyzed rainfall and temperature trends and their significance on dry cereal yield in northern Togo using the Mann-Kendall test. Fooladia et al. (2021) [23] investigated the Shahpour River in southern Iran to identify human effects and climate diversity at the river basin scale. They used Man-Kendall tests, kpss statistics, and homogeneity test at the 5% confidence level. Wenjun Huang et al. (2021) [24] used the Mann-Kendall test to determine the spatio-temporal variation of drought in northwestern China during 1950-2012 to determine the increasing or decreasing drought trend. In the present study, SPEI, NDVI, the Mann-Kendall test, and spatial statistics were used for drought analysis, and areas with high drought risk were identified. This study was conducted to identify drought behavior in the whole region under study. For this purpose, SPI and SPEI drought indices were calculated. Then, various spatial statistics, such as the mean standard deviational ellipse, the Global Moran's Index, the Anselin Local Moran, etc., were utilized to analyze the results of these indices in the GIS environment and identify the drought changes from any point to the adjacent point. These spatial statistics helped identify points that are close to each other in terms of the numerical value of drought. Areas with high numerical drought values have high-intensity droughts, which are mentioned as hot spots or high-high drought clusters. The introduced hot spots are regions from which droughts begin. The results can be used to reduce the risk of drought, identify dust centers, and planning the management of the current water scarcity problems in the area.

2. Study area

Khuzestan Province, located in the southwest of Iran and bordering the Persian Gulf, holds 80% of Iran's onshore oil reserves, thus 57% of Iran's total oil reserves. It covers an area of 63633 km2, which lies between the latitudes of 29°596 and 33°016 N and the longitudes of 46°486 and 50°306 E. The population of the province has increased from 2 million in 1978 before the revolution to 4 million in 2006, with an effective doubling of the population in less than thirty years. The elevation varies from sea level to around 3500m in the Sefid Kuh and Mangast. Further, climate conditions widely differ, although most parts of the province are arid. Parts of this region have a semi-desert climate, and other parts have a hot steppe climate. The mean precipitation is about 349 mm per year. The northern and eastern regions of the province have the maximum rate of precipitation and the lowest temperature, while the minimum precipitation and highest temperature are in the southern and western regions. The temperature difference between this province's western and eastern regions is about 7 °C, and 3 °C in the northern and southern regions. The hottest parts of this province are in the south and southwest, whereas the coldest ones are in the north and northeast. The absolute maximum temperatures in the cities of Ahvaz, Abadan, and Dezful are 50, 41, and 50 degrees, respectively, while the absolute minimum temperatures in the mentioned cities are -01, +02, and -01, respectively. The temperature usually reaches its highest and lowest points in July and February, respectively. In most parts of the province, the average annual number of sunshine hours is more than 3000 hours. Some of the critical consequences of drought and water deficits in the province involve a decline in agricultural development, the destruction of palm trees, negative impact on the lives of the residents, and most importantly, the dust crisis.

3. Material and methods

SPI:

The SPI is an index that is dependent on the probability of precipitation for each time and scale. It can be calculated for different time scales and can be an initial warning to monitor the drought and help assess its severity. This method was presented in 1993 by McKee, Doesken, and John Kleist. As members of the Colorado Center, these researchers studied different impacts of precipitation scarcity on groundwater, surface water resources, moisture content, and streamflow.

The SPI is derived from Eq. (1) [25]:

$$\mathrm{SPI} = \frac{\mathrm{P_i} - \overline{\mathrm{P}}}{\mathrm{S}} \quad (1)$$

where

$\mathrm{P_i}$: The amount of precipitation in the specified period

$\overline{\mathrm{P}}$: Long-term mean precipitation in the specified period

S: Standard deviation of precipitation value

The value of the SPI index obtained from long-term precipitation data follows a normal distribution with a mean of 0 and a standard deviation of 1. This numerical result allows examining wet and dry climates all the same.

The SPEI index is calculated using the Hargreaves-Samani method. The monthly and annual SPEI values were calculated by formulation in the Excel environment using the Hargreaves-Samani method [26] as follows:

$$\mathrm{ET0} = 0.0023\ \mathrm{Ra}\ (\mathrm{T} + 17.8)\sqrt{\mathrm{TR}} \quad (2)$$

$$\mathrm{TR} = \mathrm{T_{max}} - \mathrm{T_{min}} \quad (3)$$

where ET0 is the amount of evapotranspiration with the same unit of Ra, T is the average air temperature (°C), TR is the mean difference between the maximum and minimum temperatures (°C), and Ra is the extraterrestrial radiation (mm) of water evaporating per day for different latitudes. The SPI one-month scale indicates the drought's starting point and development better than Palmer's drought index [27]. The simultaneous use of SPI and SPEI drought indices demonstrates that the two drought indices obtain similar results [28]. SPEI is more accurate than SPI when evaporation and precipitation play an important role in drought occurrences [29]. SPI and SPEI are used to identify drought risk at the US National Drought Cessation Center, the National Aeronautics and Space Administration (NASA), the European Union Drought Center (EDC), and the Balkan Regional Meteorological Centers [30]. In this study, SPI and SPEI were selected among different drought indices, considering that precipitation variations are the main focus of drought; wet period analysis and various studies confirm the superiority of SPI over other indices in Iran. In the present study, daily statistical data (1984-2014) from 12 synoptic stations and the Water Resources Management Company (related to the Ministry of Energy) were used for the fall, winter, and early spring periods, i.e., rainfall days in Khuzestan Province (Figure 1 and Table 1). The Idnak and Pipol stations, which are adjacent to Khuzestan Province, were selected as control points for interpolation. After establishing the database in Excel 2010, SPI was computed using Drought Indices Calculator software (DIC) [31], followed by calculating drought persistence, frequency, and severity in the intended period based on this index. Thus, a background was obtained regarding the trend of drought variations in different regions of Khuzestan Province. Owing to the limitation of the required data for estimating the SPEI [32,33], the Hargreaves method, also known as the Hargreaves-Samani method [26], was utilized to compute evapotranspiration by formula writing. Numerical values created for SPI, SPEI, drought persistence, drought frequency, and drought severity during the specified period were used and transferred to the GIS environment. Then, the IDW interpolation method was selected as a fitting approach for interpolation [34-36]. The IDW method was chosen since the purpose of this study was to perform different interpolation methods using different methods of spatial statistics for drought analysis. Another reason for choosing this method was that it does not require preparation and much work on initial data. After completing the interpolation by employing spatial statistics extension in a GIS environment, we used standard deviational ellipse statistics, Anselin Local Moran index, and Getis-Ord G* to study drought behavior and identify the most crucial points whose statistics we will deal with later. Figure 2 presents a schematic diagram of the steps for a better understanding of the study.

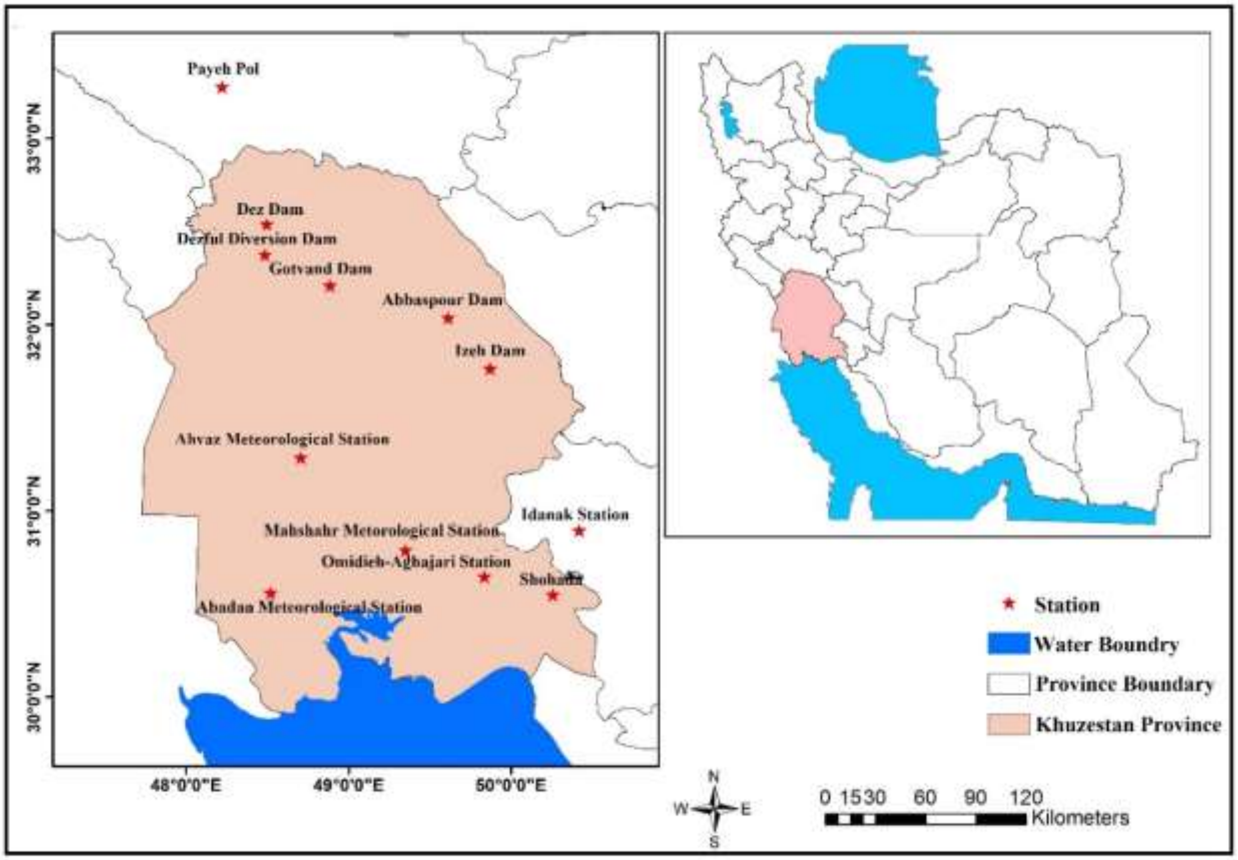

Fig. 1. The examined stations in Khuzestan Province.

Table 1. Geographical location of the examined stations.

UTM Coordinates	**Shohada Dam**	**Dez Dam**	**Izeh Dam**	**Shahid Abbaspour Dam**	**Gotvand Dam**	**Dezful Regulatory Dam**
X	428560	257875	391157	366095	295604	256914
Y	3385846	3606920	3520691	3550907	3570136	3588632
UTM coordinates	Idank Station	Pipol Station	Abadan Meteorology	Ahvaz Meteorology	Mahshahr Meteorology	Omidiyeh-Aghajari Meteorology
X	444282	231114	260239	278179	340603	387759
Y	3424207	3688939	3386859	3467526	3412319	3396658

Note. UTM: Universal Transverse Mercator.

In this part, the precipitation statistics over a 30-year period in the stations were interpolated by the IDW method in the ArcGIS environment. Also, the statistical period precipitation was divided into three decades and interpolation was arranged via the IDW method.

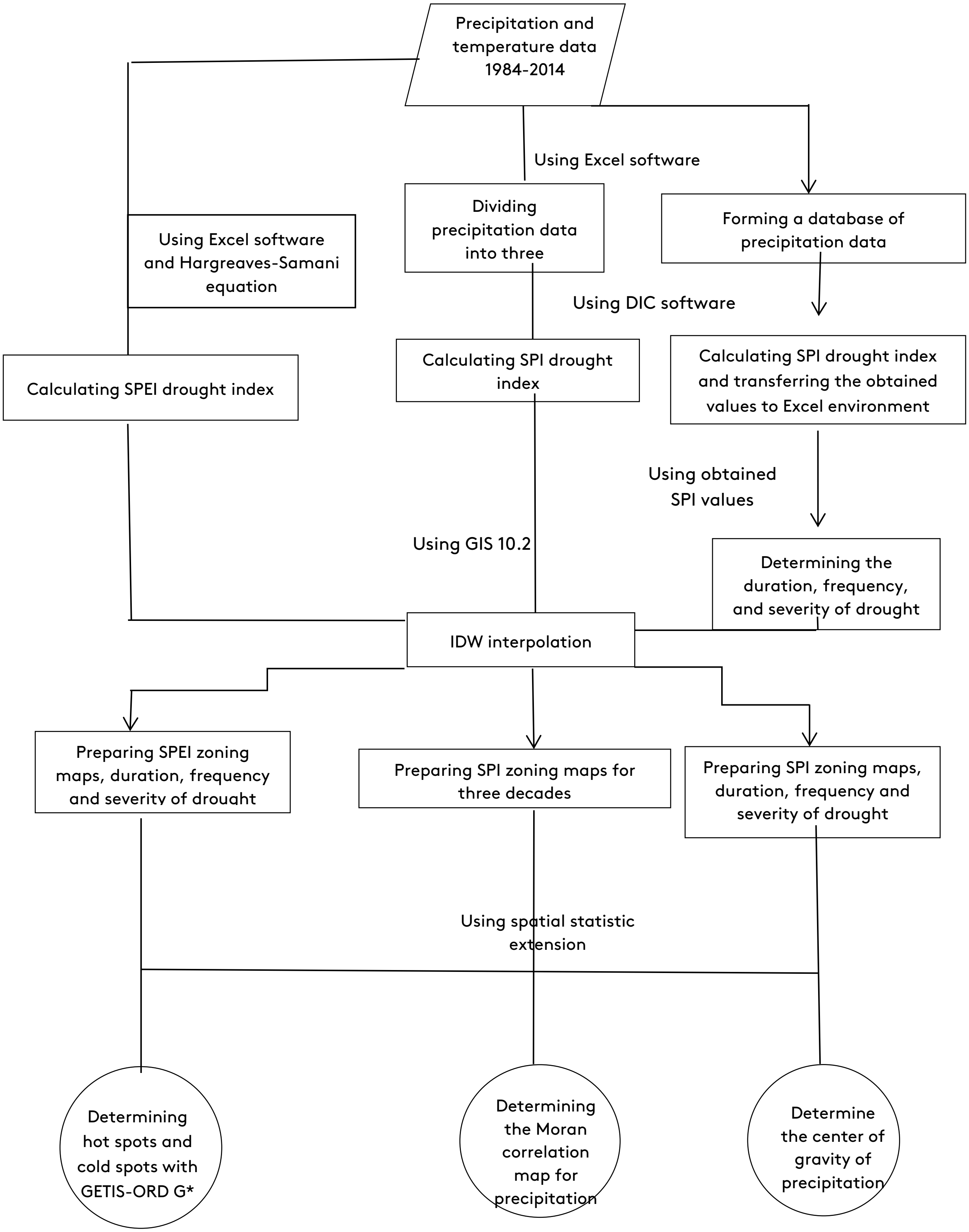

Fig. 2. Schematic figure of the steps.

3.1. The concept of spatial statistics

Spatial statistics is a branch of statistics that deals with space-dependent phenomena. A relatively significant relationship between adjacent phenomena [37] is usually expected in spatial statistics. This branch of statistics tries to make connections between different values of a variable, their distance, and orientation. This connection is called spatial structure. Location, spatial impact, and using maps are critical issues in spatial statistics. Studying the impact of one place on another is very important in spatial statistics. The basis of spatial affectivity roots back to Newton's famous equation ($\frac{m_1 m_2}{d}$) in which m_1 and m_2 are a measure of mass in places 1 and 2. Also, d is the distance between the masses. To investigate the extent and severity of drought, it is necessary to know the location of precipitation in meteorological stations in terms of length, width, and altitude. If we know these three characteristics, drought variations can be scientifically and correctly analyzed. Since station data is point-based, the information obtained from point sampling should be generalized to the study area. In this case, it is essential that we reconstruct the meteorological data status of the adjacent regions based on the data of the present stations. This course of action is conducted through the science of geostatistics and interpolation. Geostatistics is a branch of spatial statistics that uses statistical methods to find, interpolate, and extrapolate known data and estimate the value at an unknown point or unknown points. Geostatistical methods comply with statistical rules. In addition to the value of a quantity in a sample, the spatial position of the sample is considered in geostatistics. Therefore, the spatial position can be analyzed with the desired quantity value simultaneously. In other words, it must be possible to establish a connection between the various values of a quantity and their distance and orientation toward one another. This spatial relationship between the values of a quantity in the sample population may be related in mathematical formats. These mathematical forms are called spatial structures and are a function of distance and independent from coordinates [38].

3.2. Central mean and directional distribution in spatial statistics

The most renowned central tendency measure for spatial data is the central mean, which is presented as a point location in a specific study area. Analyzing the central mean in spatial statistics is similar to classical statistics, except that spatial statistics seek to obtain an equilibrium position. Hence, the geographical coordinates of the longitude points (x), latitude points (y), and sometimes altitude (Z) are of significance [39]. The directional distribution suggests the existence of a spatial trend in the features located in the study area. This trend is usually designated by a schematic ellipse called the standard deviational ellipse, whose large diameter indicates the direction of distribution [40]. The statistics of the central mean and standard deviational ellipse of precipitation are used to find the center of gravity of precipitation and zoning elongation of the precipitation values, [29,34,36]. This ellipse allows us to identify whether the distribution of features in space possesses a directional pattern. The results of determining this center can lead to identifying a new and important point for the construction of a station where rainfall is equal to the average rainfall of the whole region. The existence of such a station eliminates the need to collect rainfall information from different stations.

3.3. Spatial autocorrelation

Spatial autocorrelation is related to the relationship between residual values along the regression line. Strong autocorrelation occurs when residual values are strongly correlated; that is, changes in them occur systematically. Moran's spatial autocorrelation analysis can be used to describe the spatial properties of a variable over an entire region. It can be used to identify the mean spatial difference between all spatial features (pixels) and their adjacent features (pixels). In general, if the value of Moran's index is close to +1, the data have a spatial autocorrelation and a cluster pattern. However, if the value of Moran's index is close to -1, the data are discrete and scattered. In the case of this tool, the null hypothesis (H0) is that there is no spatial clustering between drought index values. H0 can be rejected when the P-value is too small, and the calculated

Z-value (its absolute value) is too large (outside the confidence range).

3.4. Evaluation of clusters and outliers with the Anselin Local Moran's index

Cluster and outlier analysis, also known as the Anselin Local Moran's Index, is used to show the statistical distribution of phenomena in space. Assuming we have several weighted geographic features, this tool shows where the large and small amounts of these phenomena are distributed as a cluster in space, as well as which features have very different values from the surrounding features. If the value of I is positive, it means that the desired feature (here drought) is surrounded by similar features. Therefore, the desired features are part of that cluster. If the value of I is negative, the desired feature is surrounded by features that are not similar to it at all. This type of feature is called an outlier. The Anselin Local Moran's Index can only be interpreted in terms of calculated standard score and P-Value. The output layer created by this tool includes high-value clusters (HH), low-value clusters (LL), the outlier in which a high value is surrounded by low values (LH), and outliers where a low-value feature is surrounded by high values (LH) [41,42]. Cluster and outlier analysis accomplished using the Anselin Local Moran index are helpful and highly practical tools to demonstrate the statistical distribution of phenomena in space (A and A1). In this study, Moran Local statistics were used to unveil the precipitation behavior in terms of spatial distribution patterns during the statistical period. To use this index on precipitation data, a spatial pattern that displays local differences as spatial autocorrelations on the map can be used (B1 and B). The cluster and outlier analysis, conducted by the Anselin Local Moran's index, is a useful instrument for representing the statistical distribution of phenomena in space. In this study, the Local Moran's statistic was used to determine the spatial distribution of the precipitation during the statistical period [42,43]. In this regard, the spatial pattern of local differences can be applied as spatial autocorrelation on the map.

3.5. General statistics index (G)

Moran's index is designed to describe the global spatial correlation. However, it is not efficient to identify different classification types of spatial patterns. These patterns are sometimes referred to as hot and cold spots. If high values are close to each other, Moran's index and Geary's coefficient indicate relatively high positive spatial autocorrelation. This cluster of high values may be referred to as a hot spot. However, the high positive spatial autocorrelation shown by Moran's index and Geary's coefficient may be due to low values adjacent to each other. This type of cluster is called a cold spot. Moran's index cannot distinguish between these two types of spatial autocorrelation. The general statistics index, G, is preferable to Moran's index in determining positive (hot) and negative (cold) spots in the study area. These hot and cold spots can be considered spatial concentrations [34]. Getis-Ord-Gi statistics are used when there is evidence of a clustering pattern at data collection points. However, the aim is to know whether high values lead to a clustering pattern or low values of clusters [44]. The hypothesis of a high or low clustering method is defined as follows:

Null hypothesis (H0): There is no spatial clustering in the desired variable values for the features in the study area.

The alternative hypothesis (H1): There is a high (positive) or low (negative) spatial clustering pattern in the desired variable values for the features in the study area.

The purpose of using the general statistics index, G, is to detect the presence or absence of high or low clustering in spatial data [45].

This index can be calculated using the following equation:

$$G(d) = \frac{\sum_{i=1}^{m} \sum_{j=1}^{m} \omega_{ij}(d)\, y_i y_j}{\sum_{i=1}^{m} \sum_{j=1}^{m} y_i y_j}, i \neq j \tag{4}$$

where m is the number of zones and ωij (d) is the weight based on the spatial vicinity between the regions i and j. This index measures spatial dependence using all pairs of positional values (yi, yj) so that the positions i and j are at a distance d from each other [46].

The standard score of the general statistics index, G, is measured as follows:

$$Z_G = \frac{G - E[G]}{\sqrt{V(G)}} \tag{5}$$

In a spatial pattern where the geographical location of high values is close to the position of other high values, the statistic is positive. If clustering is based on low values, the statistic is negative.

3.6. Gi index or hot spots*

The Gi* index is another spatial autocorrelation index. This index shows the distribution points of location-based data according to the type of data and spatial correlation analysis as a standard score number. This index, also known as GetisOrd G * or hot spots, can be evaluated as the following equation:

$$G_i^* = \frac{\sum_{i=1}^{n} W_{i,j}X_{i,j} - \overline{X}\sum_{j=1}^{n} W_{i,j}}{S\sqrt{\frac{\left[n\sum_{j=1}^{n} {W_{i,j}}^2 - \left(\sum_{j=1}^{n} W_{i,j}\right)^2\right]}{n-1}}} \quad (6)$$

where Xj is the attribute value for the feature j, W (i, j) is the spatial weight between the features I and j, and n is the total number of features.

$$\overline{X} = \frac{\sum_{j=1}^{n} X_i}{n} \quad (7)$$

$$S = \sqrt{\frac{\sum_{j=1}^{n} x_j^2}{n} - (\overline{X})^2} \quad (8)$$

Since Gi * is a kind of Z-score, no further calculation is needed.
The standard score classification in analyzing the type of location-based data distribution and identifying the type of clusters is according to Table 2 [34]:
parameters' needs. Therefore, the performance of any method playing a better role in refining each parameter can be a more suitable one for leachate treatment.

Table 2. Standard score classification in analyzing the type of location-based data distribution and identifying the type of clusters.

Row	Spatial distribution pattern type	p-value	(z-score)
1	Strong-cold-cold cluster	0/01	<-2/58
2	Medium-cold-cold cluster	0/05	-2/58<z<-1/96
3	Weak-cold-cold cluster	0/10	-1/96<z<-1/65
4	Random - uneven distribution	-	-1/65<z<1/65
5	Weak-hot-hot cluster	0/10	-1/65<z<1/65
6	Medium-hot-hot cluster	0/05	1/65<z<1/96
7	Strong-hot-hot cluster	0/01	>2/58

4. Results and discussion

4.1. Results relating to rainfall maps

Figure 3a-d presents precipitation maps of Khuzestan Province for three decades from 1984 to 2014 and total precipitation periods. According to the figure, the total precipitation of the first decade (1984 to 1994) shows that most of the precipitation has occurred in the northeast and northwest. In comparison, the total precipitation of the second decade (1994 to 2004) indicates that most of the precipitation has occurred in the northeast, east, and northwest. In addition, the total precipitation of the third decade (2004 to 2014) suggests that most of the precipitation has taken place in the northeast and northwest. Overall, the total precipitation of all three decades shows that most of the precipitation in Khuzestan Province occurs in the northeast, east, and northwest. From the seasonal precipitation and all three examined decades , it is inferred that the highest amount of precipitation is located in the northeastern region of Khuzestan, with the maximum precipitation being 32 mm. The total maximum precipitation in the first decade is higher than in the second decade, while it is higher in the second decade than in the third decade. Therefore, the number is decreasing as we approach 2014, i.e., the total amount of precipitation declines over time.

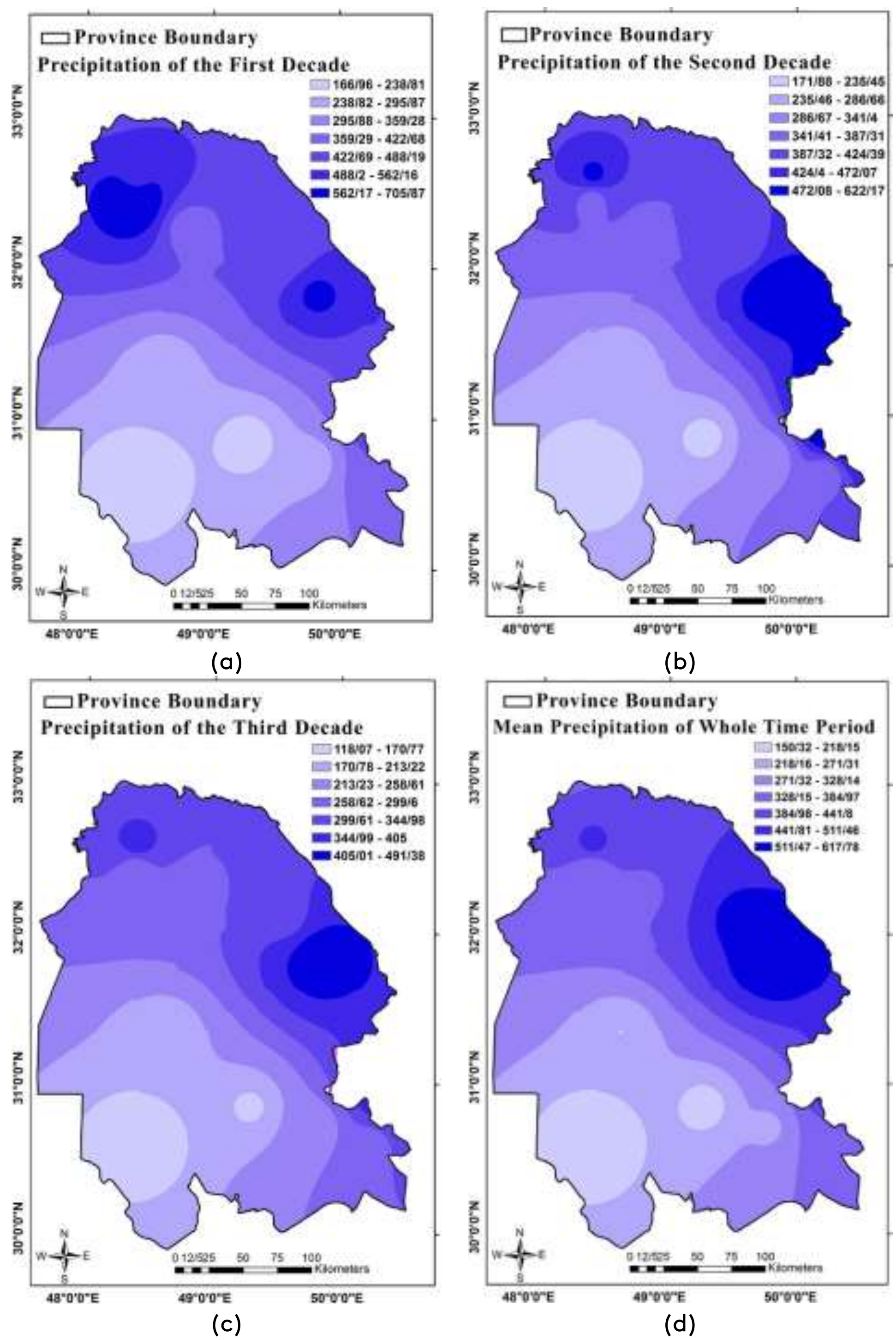

Fig. 3. Precipitation map for three decades from 1984 to 2014 and total precipitation periods. a) the first decade's precipitation, b) second decade's precipitation, c) third decade's precipitation d) the total mean precipitation of the whole examined period. Total precipitation in each decade decreases compared to the previous decade.

4.2. Results of SPI index values for the months and decades under study and the results of drought intensity in decades

As shown in Figure 4, fall and winter have similar drought situations starting in the northwest and continuing to the center and then southwest. In winter, droughts are concentrated in the central and northwestern regions of Khuzestan Province. The amount of precipitation in winter is more than in other seasons. Also, in the spring, droughts are mainly concentrated in the center to the southwest of the province. The SPI values in Figure 4 show that in the first decade (1984-1994), the droughts are more severe in the southern and southwestern regions. It can be inferred from the SPI drought maps that only the April SPI drought map corresponds to the maps of all three decades, suggesting that the majority of droughts have occurred in the southwestern regions of Khuzestan Province. Besides, the drought maps of December, January, and parts of February have similar drought zoning among the monthly SPI drought maps. In May, even though a wet year dominates in most parts of the province, the drought zoning is compatible with the drought zoning in January.

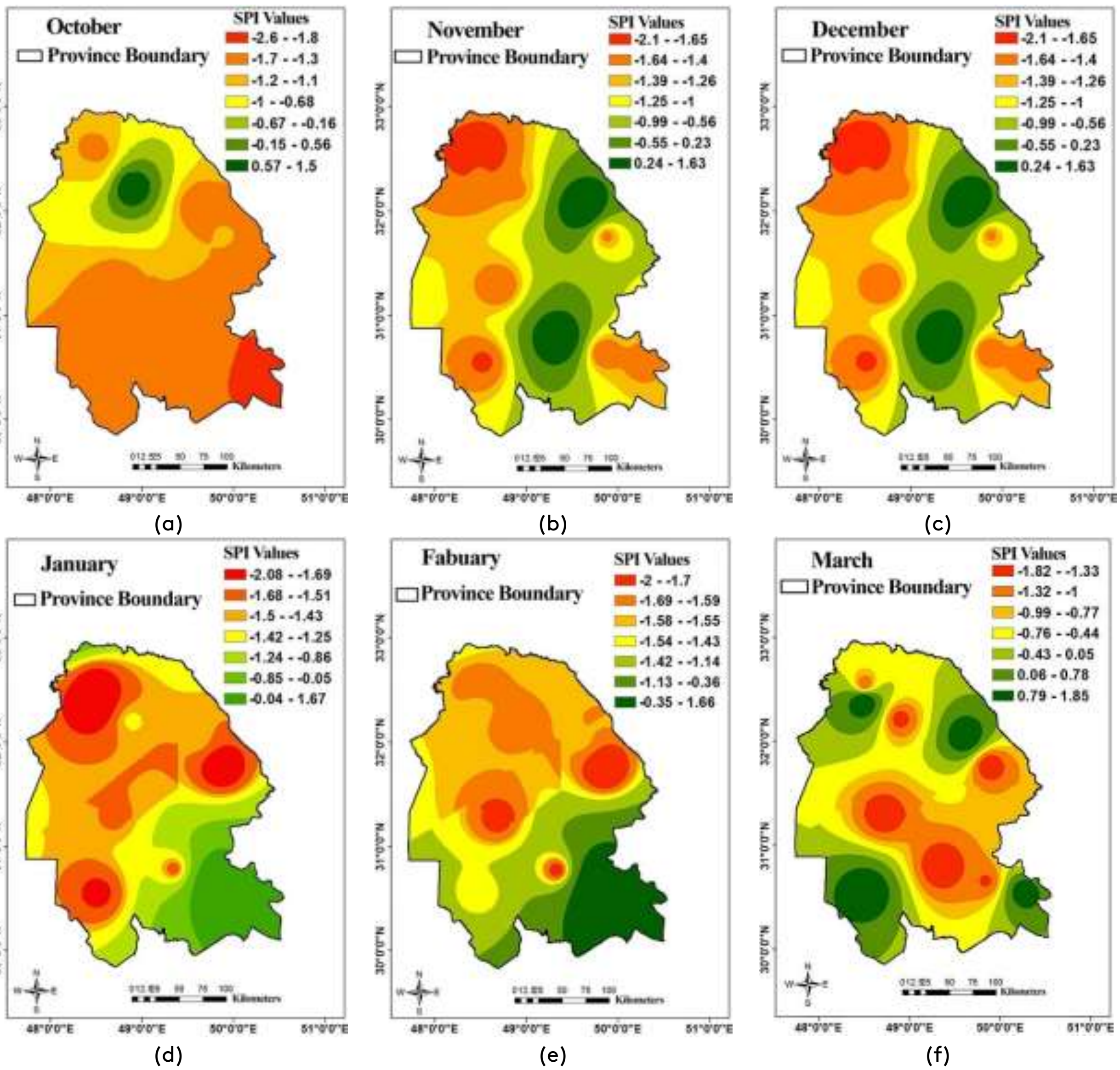

Fig. 4. Changes in SPI in the months and decades under study. a) Map of SPI changes for October, b) November, c) December, d) January, e) February, f) March, g) April, h) May, k) the map of SPI changes in the first decade, l) the second decade, m) the third decade.

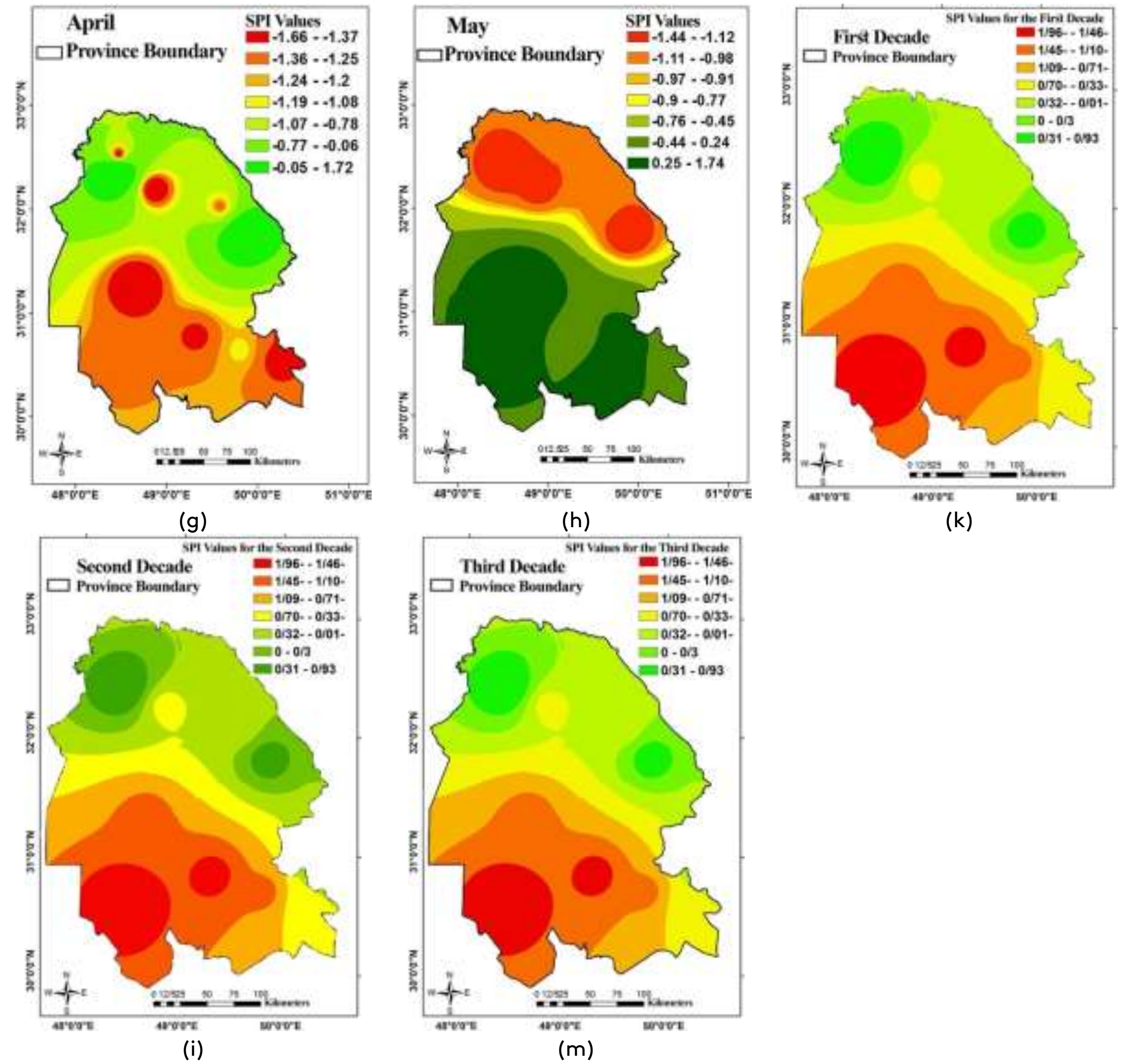

Fig. 4. Continued

Total precipitation in each decade is decreasing compared to the previous one. The extent and severity of droughts have increased from the first decade to the third decade. In Figure 5, the state of droughts determined by SPI indicates that in the first decade (1984-1994), the droughts were more severe in the southern and southwestern regions of Khuzestan Province. The severest droughts have occurred in the southwest in the first decade, but there is no remarkable change in the second decade. In the third decade, while the extent of droughts increased, quite severe droughts also emerged in the southwest.

Note. SPI: Standardized Precipitation Index.

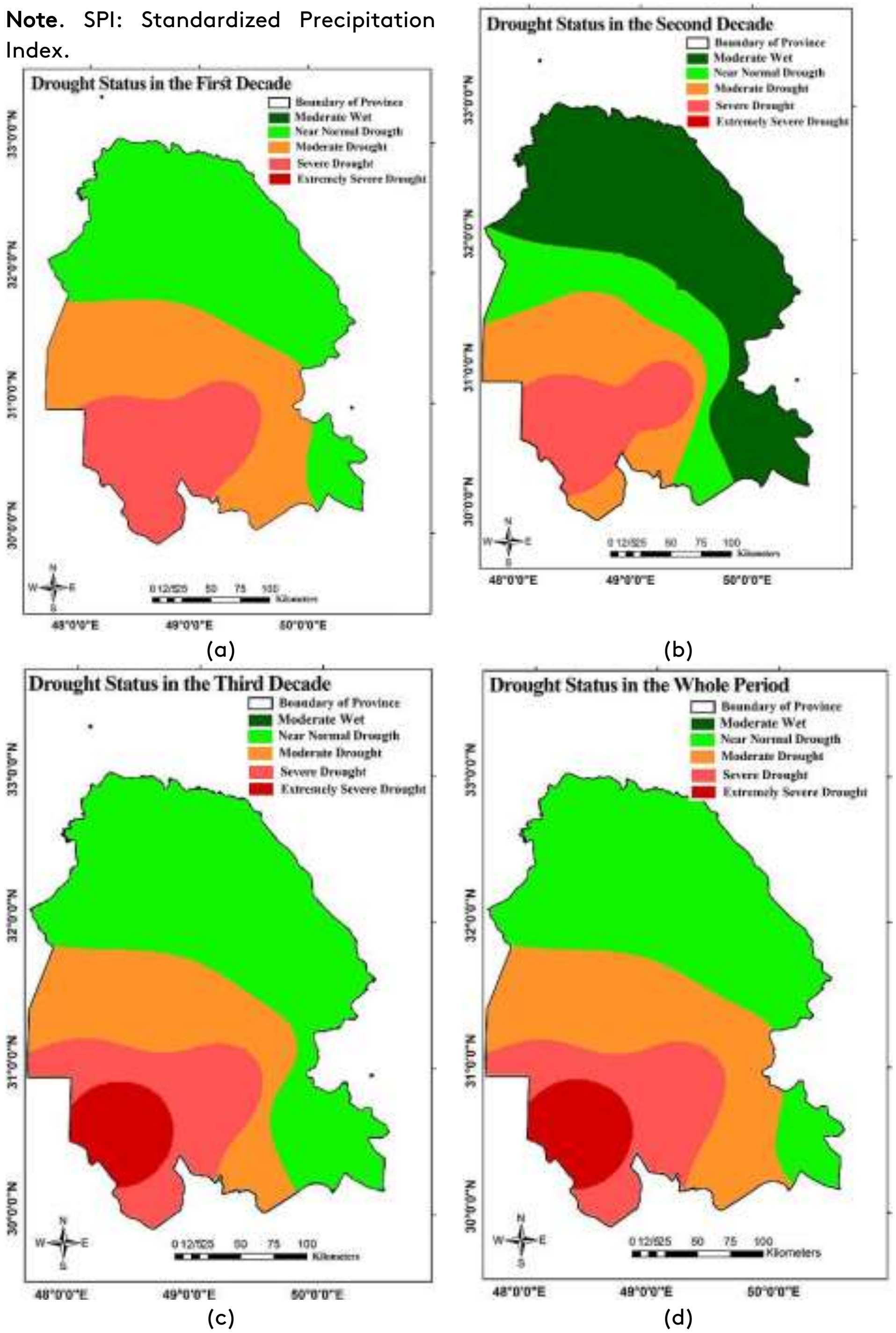

Fig. 5. Drought status in the examined decades based on the SPI. a) drought conditions of the first decade, b) second decade, c) the third decade, d) the whole period's total drought.

4.3. The initial assessment of the duration, severity, and frequency of droughts based on determined SPI values

After determining the drought conditions using the SPI index, the drought continuity and magnitude of the stations were examined. These results are presented in Table 3 from right to left. The longest drought continuity of each station is presented in the second column of the table. Then, the months and years in which this continuity occurred are shown in the third column of the table. Given the frequency of drought continuities, the number of drought continuities for the stations is indicated in the fourth column. Based on the reported continuities in the fourth column, the month with greater continuity is specified in the fifth column.

For the periods of drought continuity and the month mentioned in the fourth and fifth columns, the maximum drought magnitude is reported in the sixth column. The year related to the number of drought magnitude reported in the sixth column is presented in the seventh column. For example, in the first row of the table, the Shohada Dam has the longest continuity, with five consecutive years of drought occurring in March of each year from 2005-2009. Moreover, during the period under study, this station had four periods of drought continuity, occurring mostly in November. Furthermore, the maximum amounts of drought magnitude in these four periods are -14.7, -23.6, -24, and- 24 occurring in 1987, 1998, 2003, and 2007, respectively. The most severe droughts were observed at Shahid Abbaspour dam station from 1989 to 1997 and 2011. The statistics on drought frequency indicate that the highest frequency was for November, with 30-50% in the southeastern regions of Khuzestan Province. The southern regions of Khuzestan Province have a higher drought recurrence, with a drought frequency of 30%.

Table 3. Results of the initial assessment of the duration and severity of the drought based on the determined SPI values.

The year with the severest drought	The severest drought in consecutive durations	The month with the most consecutive drought duration	The number of consecutive drought durations	Months and years with the longest drought durations	The longest consecutive drought durations	Station
1987 1998 2003 2007	-14.7 -23.6 -24 -24	November	4 periods	2005-2009 March	5 years	Shohada Dam
2008 2014 1986 2008	-19.1 -44.1 -52.9 -60.6	February January	2 periods	1998-2000 April	3 years	Dez Dam
2003 2007	-64.73 -65.53	March	2 periods	2005-2008 March	4 years	Izeh Dam
1989 1997 2011	-79.7 -79.7 -79.2	November and December	3 periods	1988-1990 May	3 years	Shahid Abbaspour Dam
The same The same	-11.1 -11.1	May	3 periods	2010-2012 April	4 years	Gotvand Dam
The same 1998	-13.4 -13.4	May	2 periods	1989-1990 May	2 years	Dezful Regulatory Dam
1989 1987 1990	-22.5 -23.5 -20.9	January	3 periods	November-January-February A 2-year period	2 years	Abadan Meteorology
1987 1994 2009	-32.01 -13.21 -28.41	December	3 periods	1999-2001 April	3 years	Ahvaz Meteorology
1986 1989 2010	-31.54 -20.4 -26.4	December	3 periods	1999-2001 April	2 years	Mahshahr Meteorology
1984 2004 2013	-16.68 -22.23 -16.63	March	3 periods	March	2 years	Omidiyeh-Aghajari

4.4. Analysis of drought maps based on the SPEI

The SPEI drought maps prepared via the geostatistical method demonstrated that all regions of Khuzestan Province experienced droughts in November. In December and February, only the southern and southwestern regions experienced droughts. In January, no drought occurred. In March, all the regions experienced drought, except for some parts of the northwest and northeast. In April, all the regions, except for parts of the northeast, experienced a drought. In May, severe droughts occurred in the north and northeast of Khuzestan, while most other regions experienced moderate droughts (Figure 6). In the drought maps, the second and third decades were more analogous. There was a wet season near Shohada Dam station in the first decade, while the southern regions experienced a severe drought. Compared to the first period, the northern region shifted from a wet season to nearly normal in the second and third decades. In the third period, some areas of the northwest shifted from nearly normal to moderate drought. Finally, the southern regions were alike in the second and third periods.

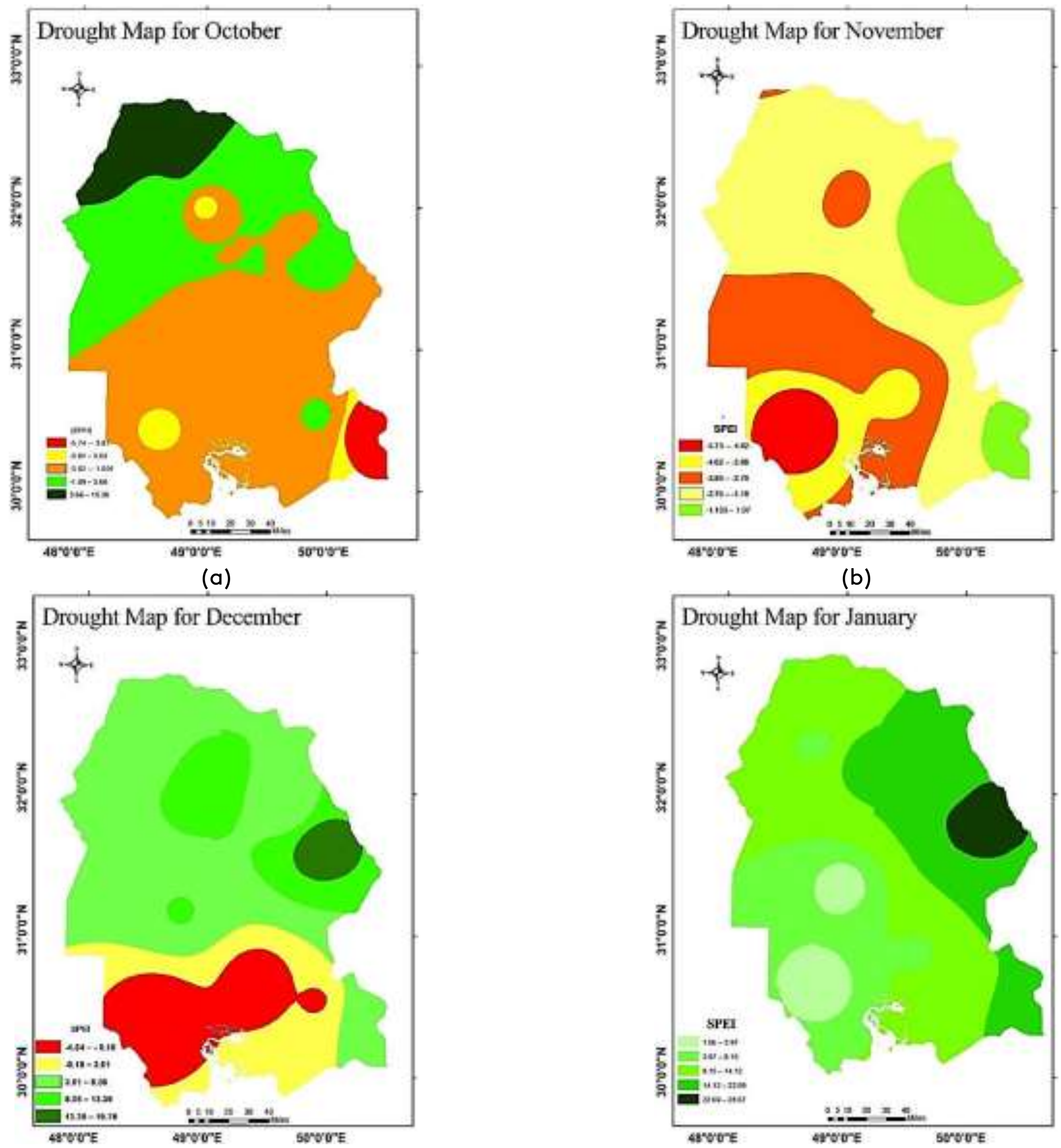

(c) (d)

Fig. 6. Drought maps of the examined months based on the SPEI. The map of SPEI variations in a) October, b) November, c) December, d) January, e) February, f) March, g) April, h) May
SPEI: Standardized precipitation-evapotranspiration index

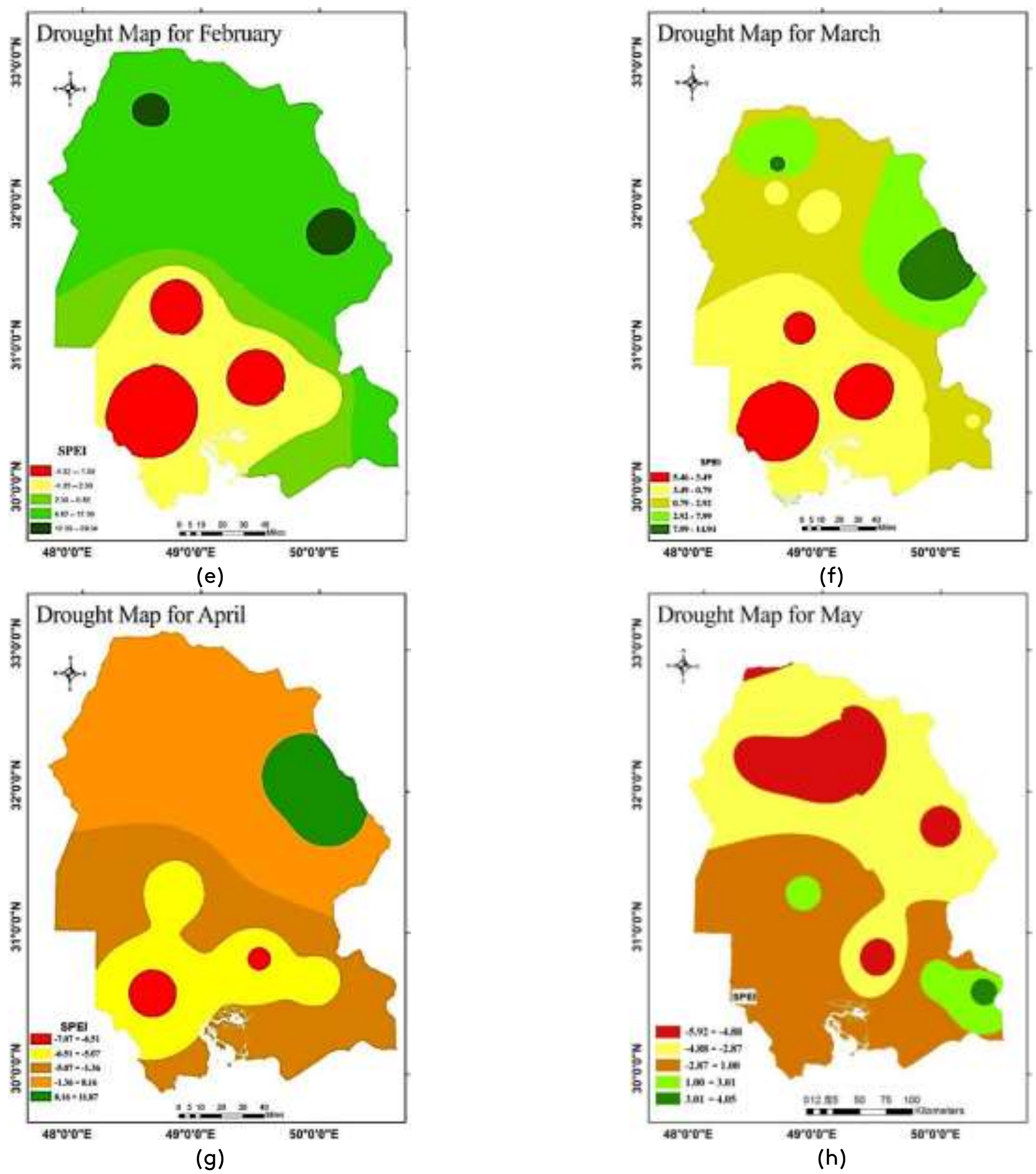

Fig. 6. Continiued

.

4.5. Results of drought analysis through spatial statistics

4.5.1. Description of the mean precipitation and standard deviational ellipse

Standard deviational ellipse statistics were used to find the center of gravity of the precipitation and the elongation of precipitation values. As shown in Figure 7, the central mean and standard deviation of the annual and decadal precipitation in the Khuzestan region is located in the center of the map. The mean precipitation center of all stations, both in the statistical period under study and the decadal periods, is located in the center of Khuzestan. The gravity center of annual precipitation and decadal precipitation is located in the center of the Khuzestan map. Here, the standard deviational ellipse, which elongates from northwest to southeast at 68.26%, shows data dispersion toward the central mean point of annual and decadal precipitation in an almost fixed position.

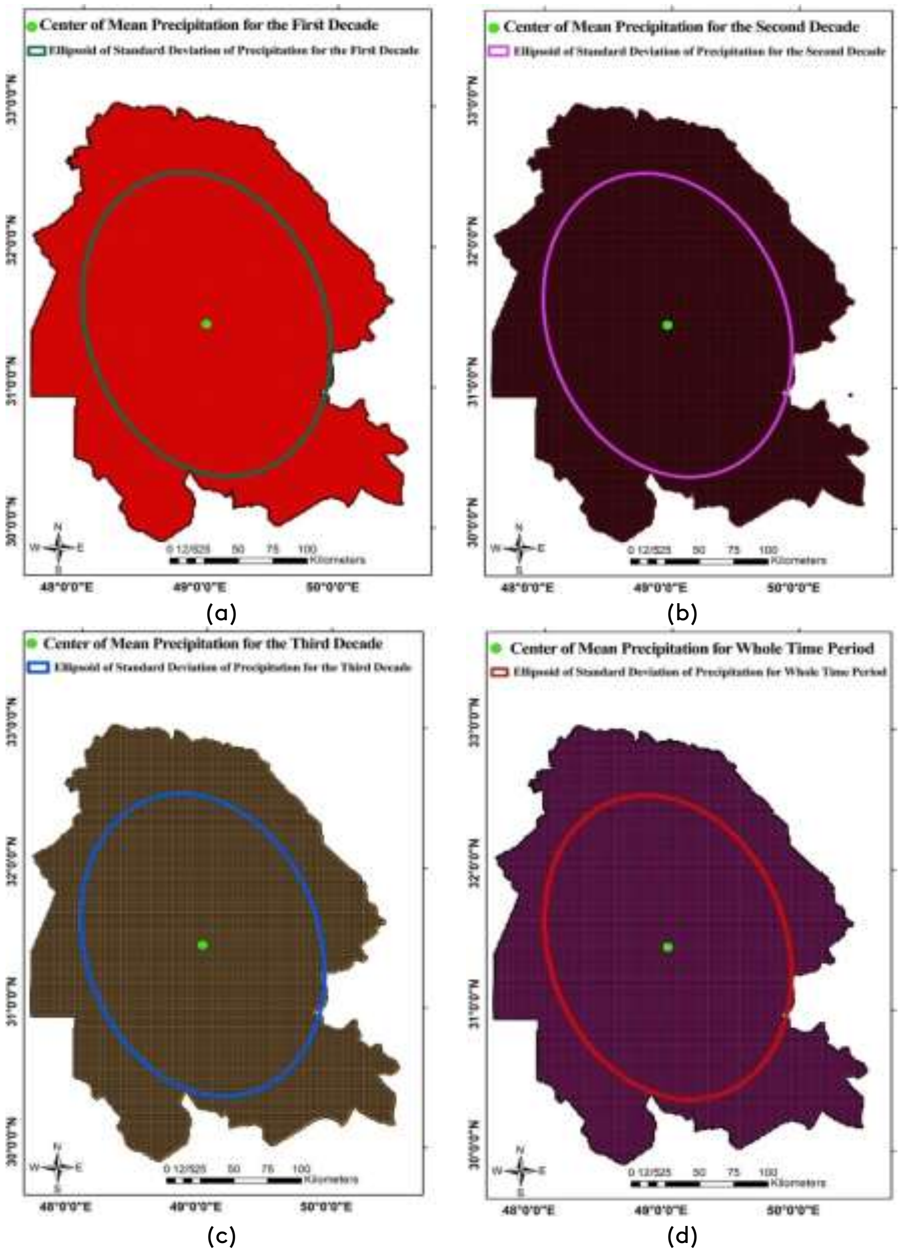

Fig. 7. Mean points of the three decades in 1984-2014 and the mean of all periods with the standard deviational ellipse.The image of the mean precipitation center and the standard deviational ellipse of the a) first decade, b) the second decade, c) the third decade, d) the total of the whole examined period the mean precipitation and the standard deviational ellipse in all three decades are in an almost fixed position.

4.5.2. Results of Anselin Local Moran statistic to identify the clusters based on SPI

Figure 8 presents the spatial autocorrelation maps of Anselin Local Moran in the studied months. As can be seen, the high-high clusters of precipitation are generally located in the northeastern regions of Khuzestan in the statistical period. The high-high clusters that appear in May have an entirely different appearance from other wet seasons in Khuzestan because they have risen in the southeastern and southwestern regions of Khuzestan. No high-low or low-high cluster patterns appear in the maps of the mentioned months. These patterns are not statistically significant and are distributed as gray dots on the map. Throughout the entire study period and each of the examined decades, high-high precipitation clusters are located in the northeastern region of Khuzestan. Maps of all three decades reveal that clusters show almost the same behavior in all three decades.

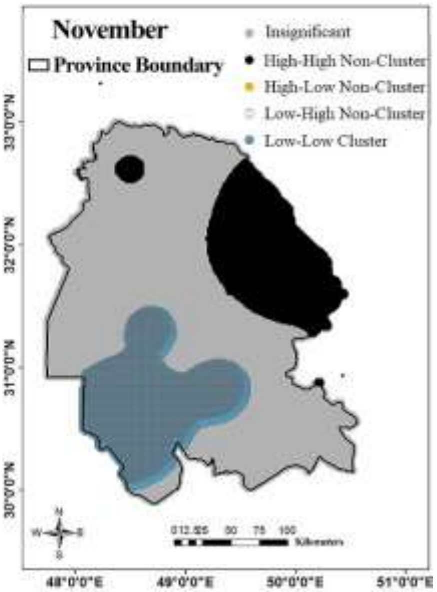

(a)

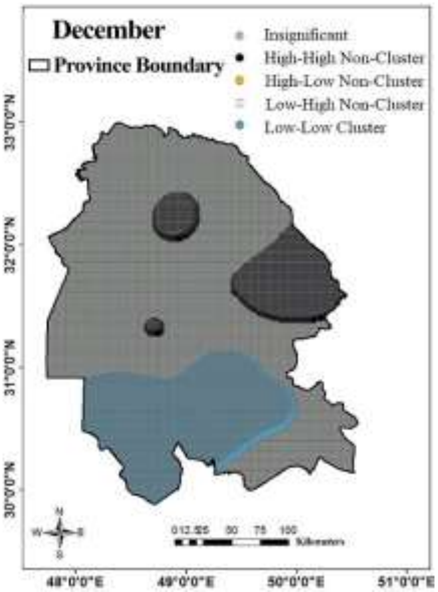

(b)

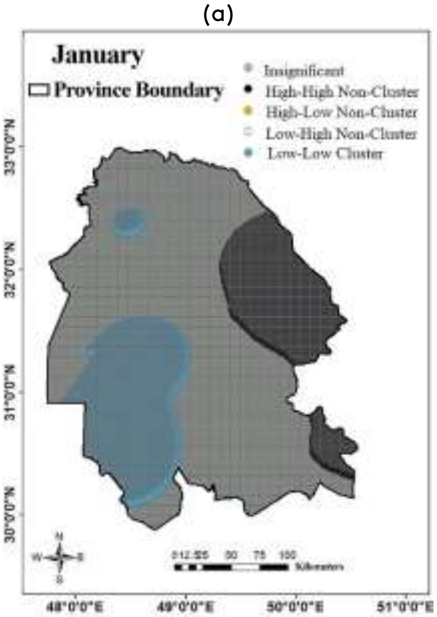

(c)

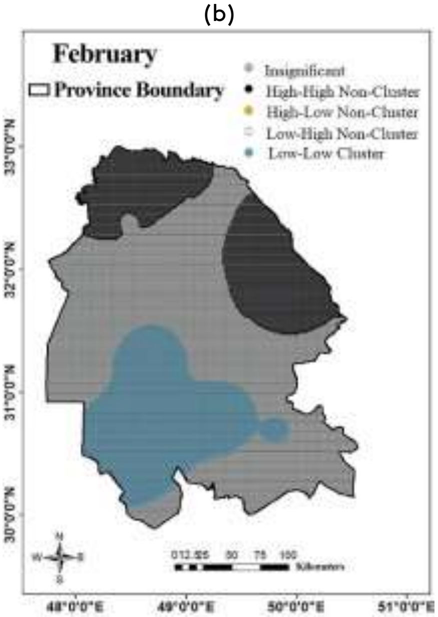

(d)

Fig. 8. Moran's spatial autocorrelation map for the examined months and decades. Moran's precipitation correlation maps for a) November, b) December, c) January, d) February, e) March, f) April, g) May, h) Provide the maps of the h) first, i) second, j) third decade, k) finally all three decades.

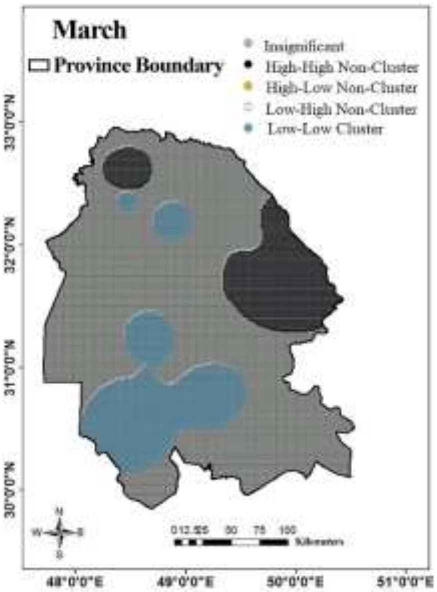

(e)

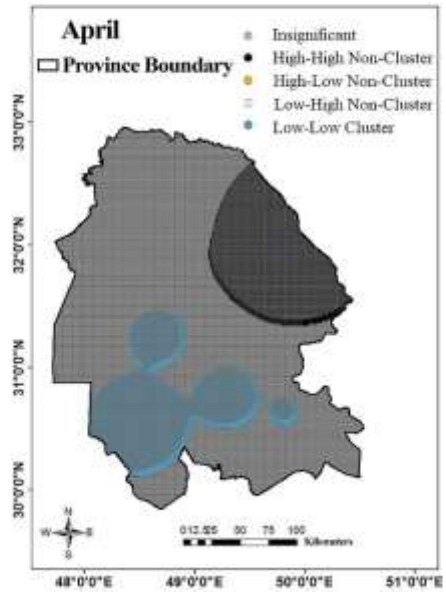

(f)

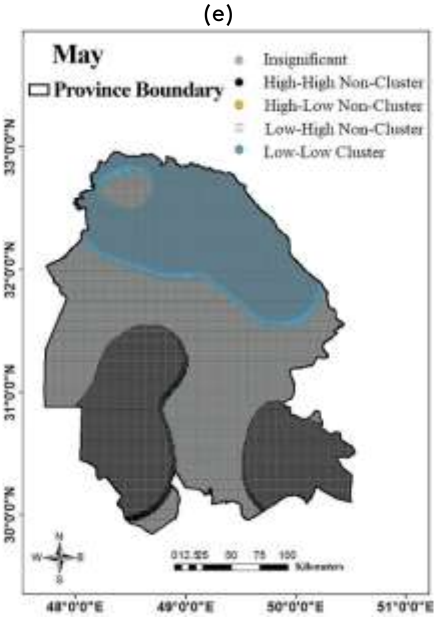

(g)

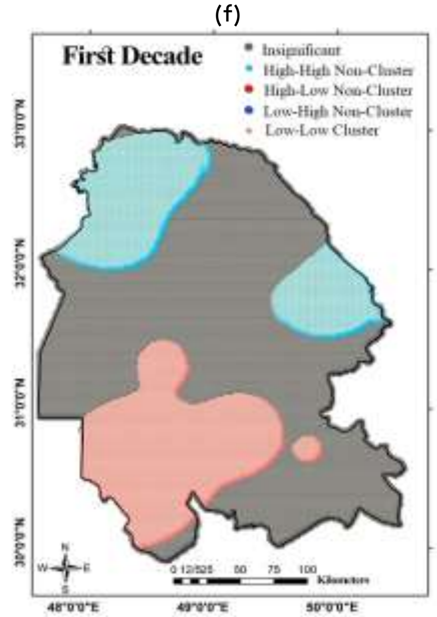

(h)

Fig. 8. Continued

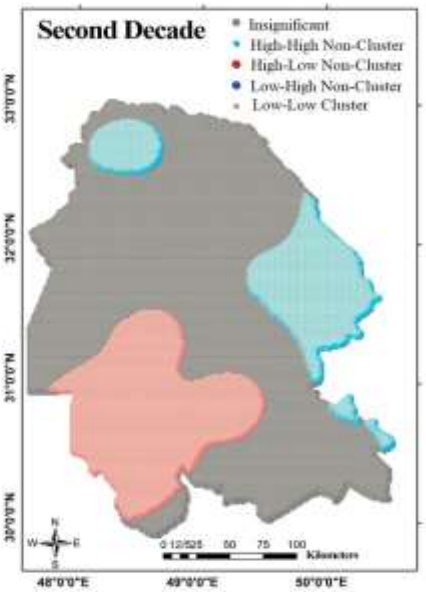

(i)

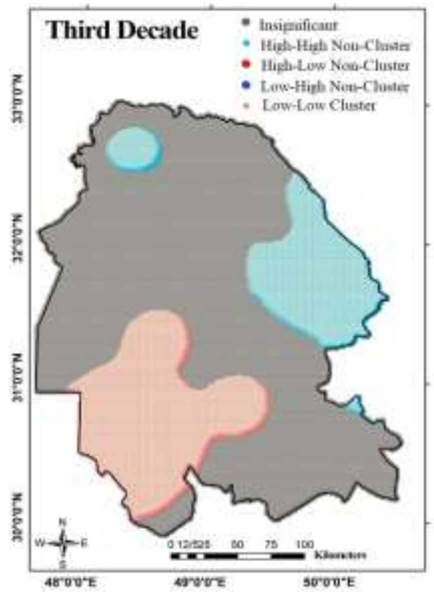

(j)

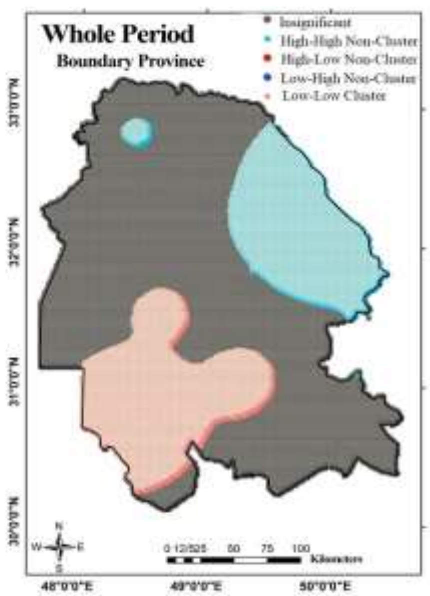

(k)

Fig. 8. Continued

4.5.3. Results of Getis-Ord G statistic to identify the hot and cold spots based on SPI*

According to the map of hot spots in November, the high-high drought clusters were located in the southern and southwestern regions of Khuzestan Province on the Persian Gulf. The concentration of clusters with relatively lower values than high clusters was also seen in this part with a lighter red color (Figure 9). Therefore, in November, hot spots formed from Abadan and Shadegan to Bandar Mahshahr and continued to Ahvaz. Cold spots, which indicate clusters with low drought values, were located in the northwestern region of Khuzestan Province. The results of the drought state for this month were compatible with those of Anselin Local Moran precipitation (Figure 8). In December, the drought cold spot, which holds clusters with low drought values, was placed as a small spot in the northwest. Another cold spot was placed between the south and southeast of Khuzestan. This spot was significant with a 90 to 99% confidence level, suggesting cluster formation with low drought values. In this month, only a very small hot spot could be observed in the northern region of Khuzestan, indicating a favorable situation regarding the absence of drought. At other stations, there was no significant relationship between SPI values. Moreover, there was no significant relationship between SPI values in other stations. In January, hot spots with high drought values only appeared in the southeastern region of Khuzestan. They were also seen in its borders with relatively lower values of droughts, suggesting the formation of clusters with high drought values in the southeastern region of Khuzestan.

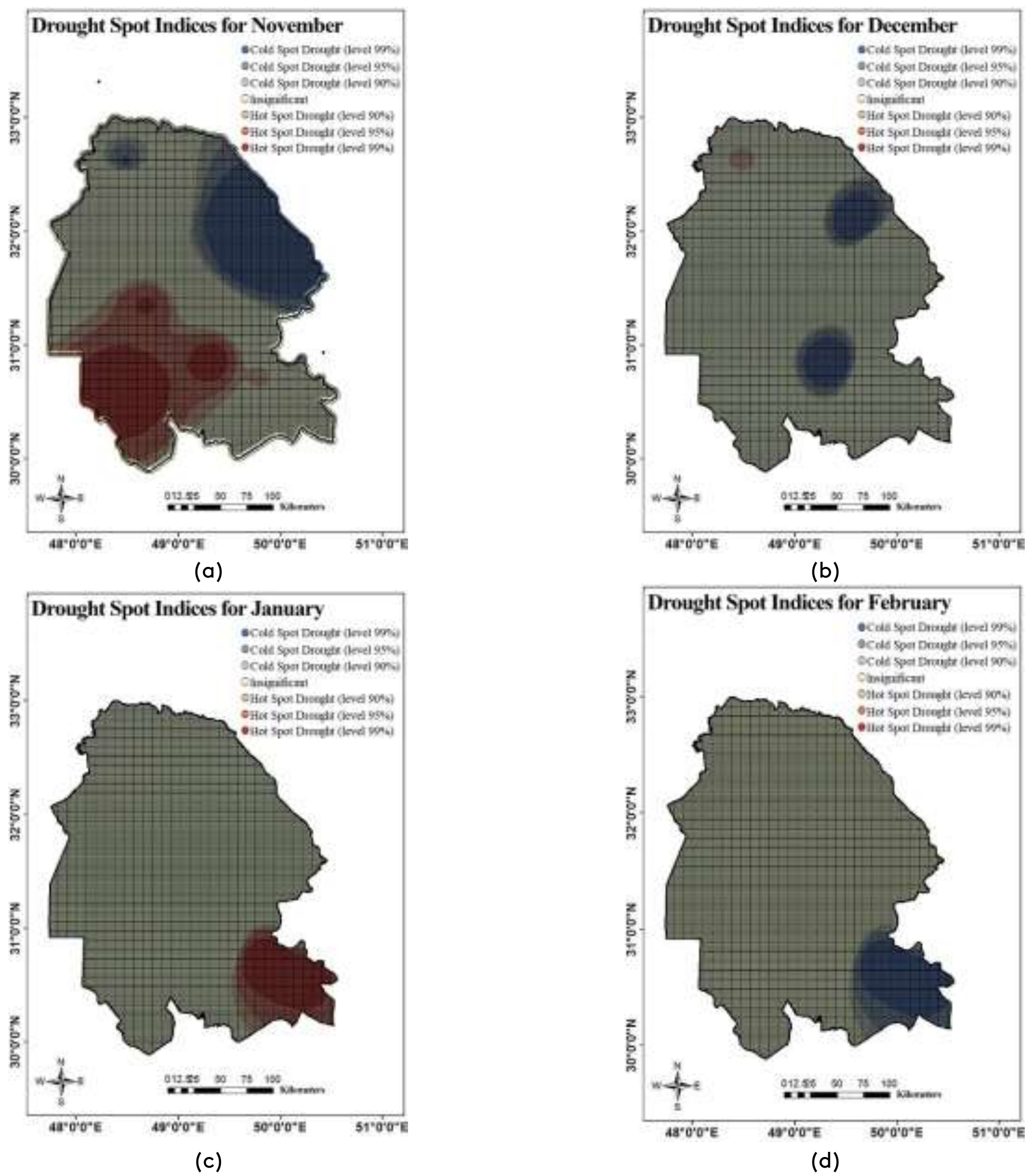

Fig. 9. The map of hot and cold spots in the intended months based on the SPI. The hot spot and cold spot maps for a) November, b) December, c) January, d) February, e) March, f) April, g) May.

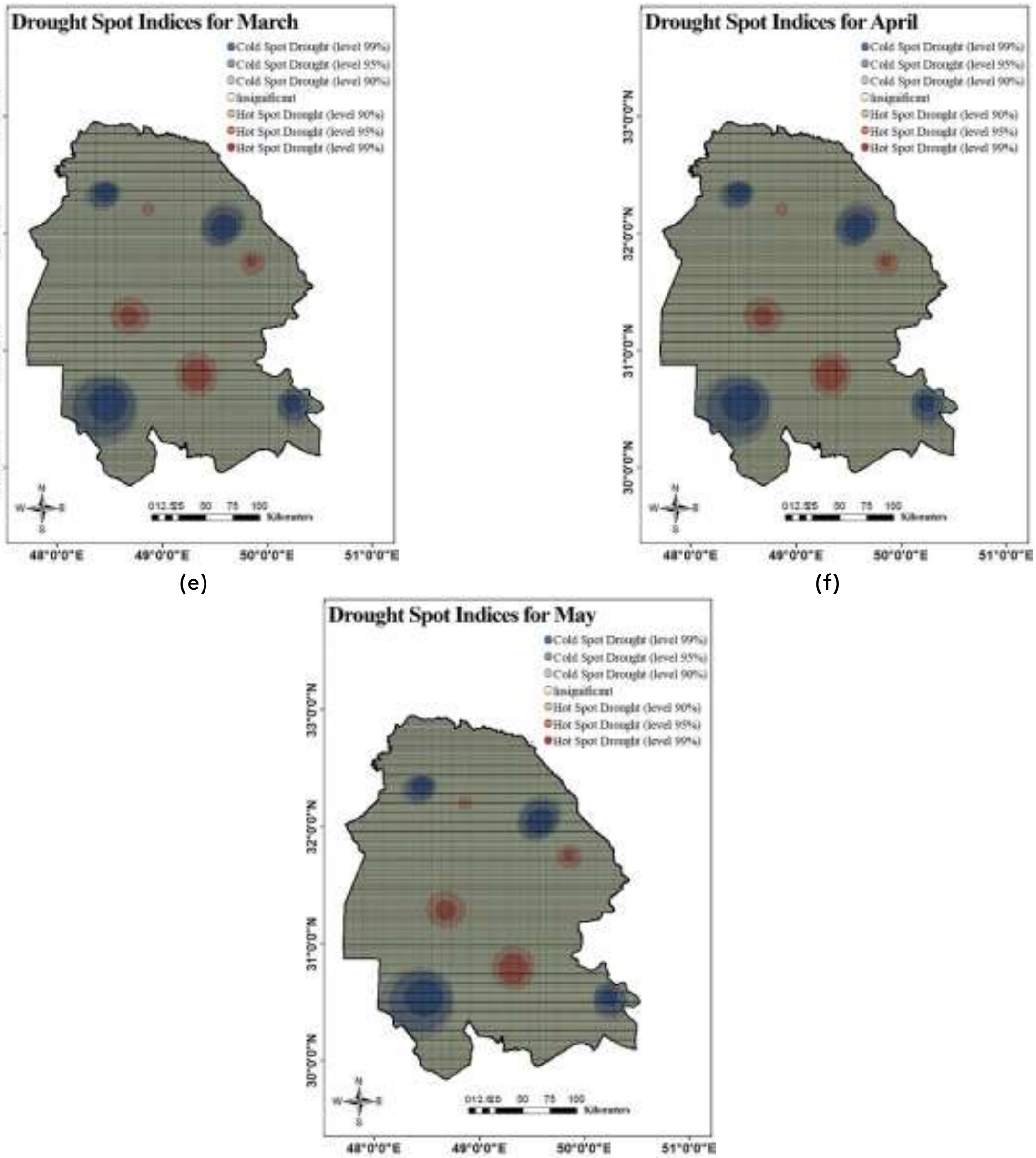

(e) (f) (g)

Fig. 9. Continued

Table 4. The hot spots and cold spots formed in the stations according to SPI and confidence level value.

STATION	November	December	January	February	March	April	May
SHOHADA Dam	-	-	Hot spot 99%	Hot spot 99%	Hot spot 99%	Cold spot 99%	Cold spot 99%
DEZ Dam	Cold spot 90%	Hot spot 90%	-	-	-	-	-
IZEH Dam	Cold spot 99%	Cold spot 90%	-	-	Hot spot 99%	Hot spot 99%	Hot spot 99%
ABBASPOOR Dam	Cold spot 99%	Cold spot 99%	-	-	Cold spot 99%	Cold spot 99%	Cold spot 99%
GOTVAND Dam	Cold spot 99%	-	-	-	-	-	-
DEZFOOL DIVERSION Dam	Cold spot 99%	-	-	-	Cold spot 90%	Cold spot 99%	Cold spot 90%
ABADAN	Hot spot 99%	-	-	-	Cold spot 99%	Cold spot 99%	Cold spot 99%
AHWAZ	Hot spot 90%	-	-	-	Hot spot 99%	Hot spot 99%	Hot spot 99%
MAHSHAHR	Hot spot 90%	-	-	-	Hot spot 99%	Hot spot 90%	Hot spot 90%
OMIDIYEH-AGHAJARI	Hot spot 99%	-	Hot spot 90%	Hot spot 99%	-	-	-

4.5.4. Results of clustering and analysis of hot and cold points based on SPEI

According to the map in Figure 10b of hot spots in November, the high-high drought clusters are located in the southern and southwestern regions, and a small spot is placed in the northern region. The clusters with relatively lower values are concentrated around the central region and Ahvaz. Therefore, in November, hot spots have formed from Abadan and Shadegan to Bandar Mahshahr, proceeding to Ahvaz. Cold spots are seen in the northeastern and southeastern borderline, and there is a small spot near the Dezful Regulatory Dam. In December, cold spots cover a large region from the center to the north of Khuzestan, and hot spots cover a large area from the center to the south. It is noticeable that the borderline between these two spots is non-significant. In January, there were hot spots with high drought values in the eastern half of Khuzestan. The western half of Khuzestan primarily contained cold spots. In February, this pattern was reversed in January, i.e., the hot spots were discovered in the western regions of Khuzestan as a line, while the cold spots were present from north to south in the eastern half of the province. In March, hot spots in the western half and cold spots in the eastern half spread from north to the northeast (near Izeh Dam). In April, hot spots appeared in the northern regions, proceeded to the Gotvand Dam stations, and reached the east of Khuzestan. Meanwhile, cold spots of drought covered all the central regions to the south of Khuzestan. In May, hot spots of drought spread from the northeast to the northwest of the province. A small hot spot was also identified near the Mahshahr station in the southwest of Khuzestan. In this month, the cold spots were concentrated in the southeastern and southwestern regions of Khuzestan. These two regions connected in light blue hold lower drought values and have a confidence level of 90%.

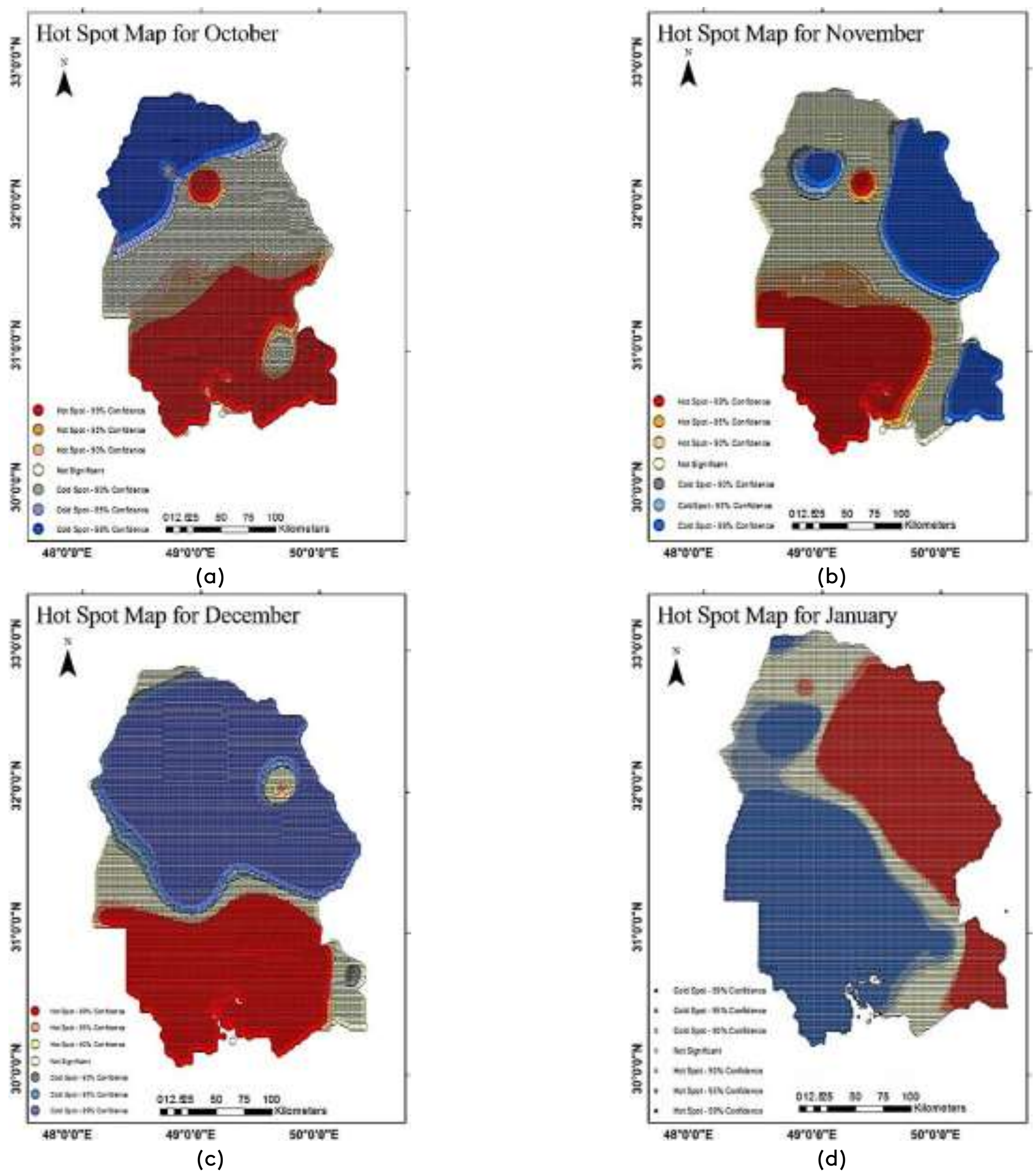

Fig. 10. The map of hot and cold spots in the examined months based on the SPEI. The map of hot spots and cold spots in a) October b) November c) December d) January e) February f) March g) April h) May.
SPEI: Standardized precipitation-evapotranspiration index.

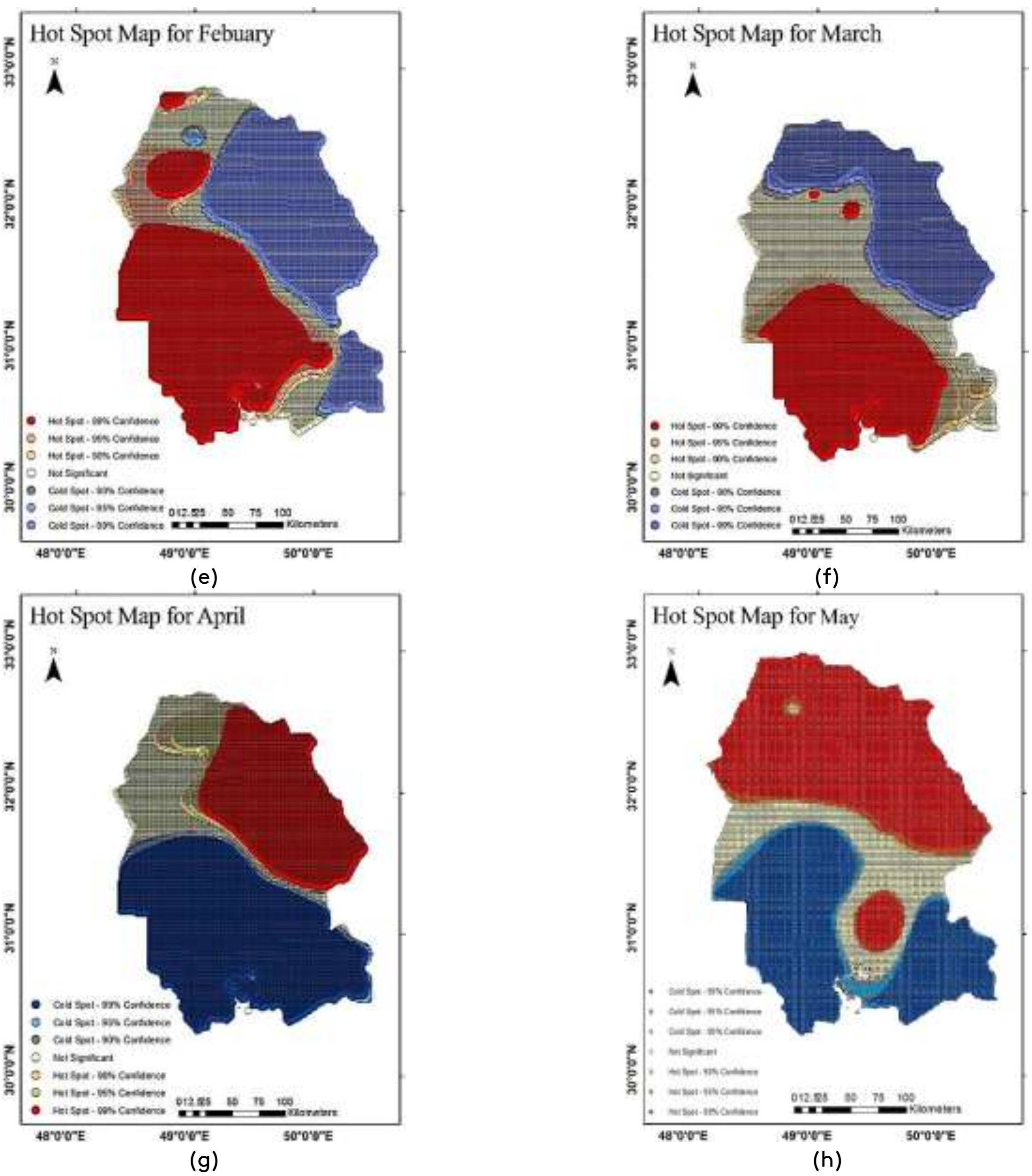

Fig. 10. Continued

Table 5. The results of the formed hot spots and cold spots according to SPEI and the respective confidence levels.

STATION	October	November	December	January	February	March	April	May
SHOHADA Dam	Hot spot 99%	Cold spot 99%	-	Hot spot 99%	Cold spot 99%	Hot spot 90%	Cold spot 99%	Cold spot 90%
DEZ Dam	Cold spot 95%	-	Cold spot 99%	-	-	Cold spot 99%	Hot spot 90%	Cold spot 99%
IZEH Dam	-	Cold spot 99%	Cold spot 99%	Hot spot 99%	Cold spot 99%	Cold spot 99%	Hot spot 99%	Cold spot 99%
ABBASPOOR Dam	-	Cold spot 99%	Cold spot 99%	Hot spot 99%	Cold spot 99%	Cold spot 99%	Hot spot 99%	Cold spot 99%
GOTVAND Dam	Cold spot 99%	Cold spot 90%	Cold spot 99%	Cold spot 99%	Hot spot 99%	Hot spot 99%	Hot spot 99%	-
DEZFOOL DIVERSION Dam	Cold spot 99%	Cold spot 990%	Cold spot 99%	Cold spot 99%	Hot spot 99%	Cold spot 99%	Hot spot 90%	-
ABADAN	Hot spot 99%	Hot spot 99%	Hot spot 99%	Cold spot 99%	Hot spot 99%	Hot spot 99%	Cold spot 99%	Hot spot 99%
AHWVAZ	Hot spot 95%	Hot spot 90%	Cold spot 99%	Cold spot 99%	Hot spot 99%	Hot spot 99%	Cold spot 99%	Hot spot 99%
MAHSHAHR	Hot spot 99%	Hot spot 99%	Hot spot 99%	Cold spot 99%	Hot spot 99%	Hot spot 99%	Cold spot 99%	Hot spot 99%
OMIDIYEH-AGHAJARI	Hot spot 95%	-	Hot spot 99%	Cold spot 99%	Hot spot 99%	Hot spot 90%	Cold spot 99%	Hot spot 99%

4.5.5. Drought comparison of the three decades according to hot spot maps

The hot spot maps are similar in the three studied decades. The results of this analysis are significant, with a 99% confidence level in the meteorological stations in the following locations: Abadan, Ahvaz, Mahshahr, and Omidiyeh Aghajari; they all were following a severe drought pattern. Hot spots formed in the center (Ahvaz) to the southeast (Omidiyeh and Aghajari) and the west of Khuzestan. For the northern and northwestern stations (Dezful Dam, Dez Dam, and Gotvand Dam), which were nearly normal, hot spots were recognized to be 99% significant. In Shahid Abbaspour Dam and Dez Dam stations, which experienced a wet season, cold spots were identified with a confidence level of 99%. In all three decades, the drought cold spots spread from the north to the east of Khuzestan. The Shohada Dam station was recognized as non-significant in terms of hot spots or cold spots in statistical decades.

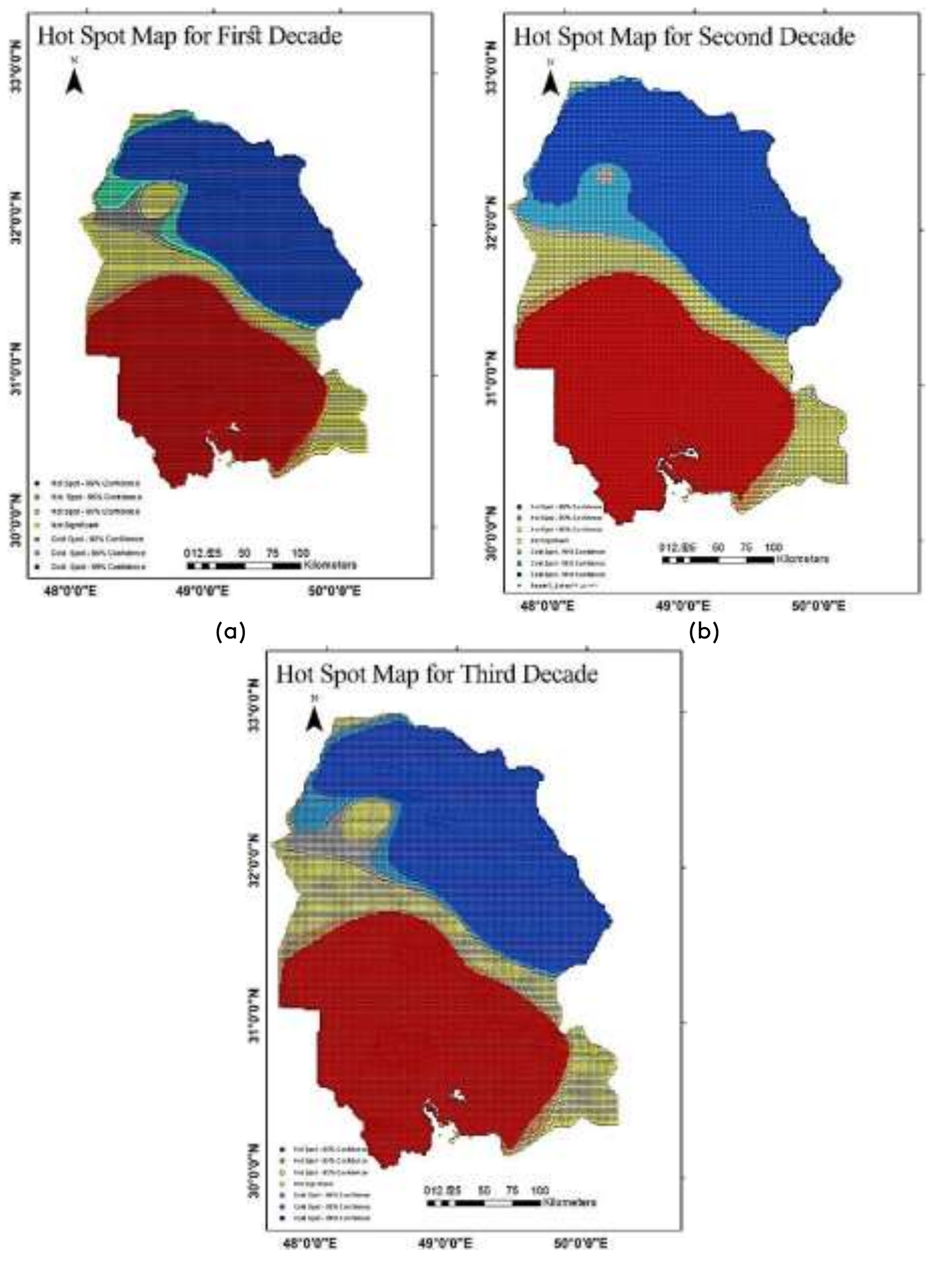

(a) (b)

(c)

Fig. 11. The map of hot and cold spots in the examined decades based on the SPEI. Hot spot and cold spot maps in the a) First, b) Second, c) Third decades.
SPEI: Standardized precipitation-evapotranspiration index.

4.5.6. Interpreting the local Moran's map of droughts in all three decades

The high-high drought clusters denote the parts of the study area with greater drought values over the decades. On the other hand, the low-low clusters show the parts with lower drought values over three decades. The other parts for which no cluster has been identified have had very different drought values from the adjacent points. Moreover, non-cluster of the L-H or H-L types has not been identified. Local Moran's maps of drought are closely alike in all three decades. In all three decades, high-high drought spots are located in the southern and southwestern regions of Khuzestan, while low-low drought spots are located in the northern and northeastern regions of Khuzestan (Figure 12). The recurrence of the high-high clusters in all three decades shows that the drought condition has remained constant from the southwestern to the southeastern parts.

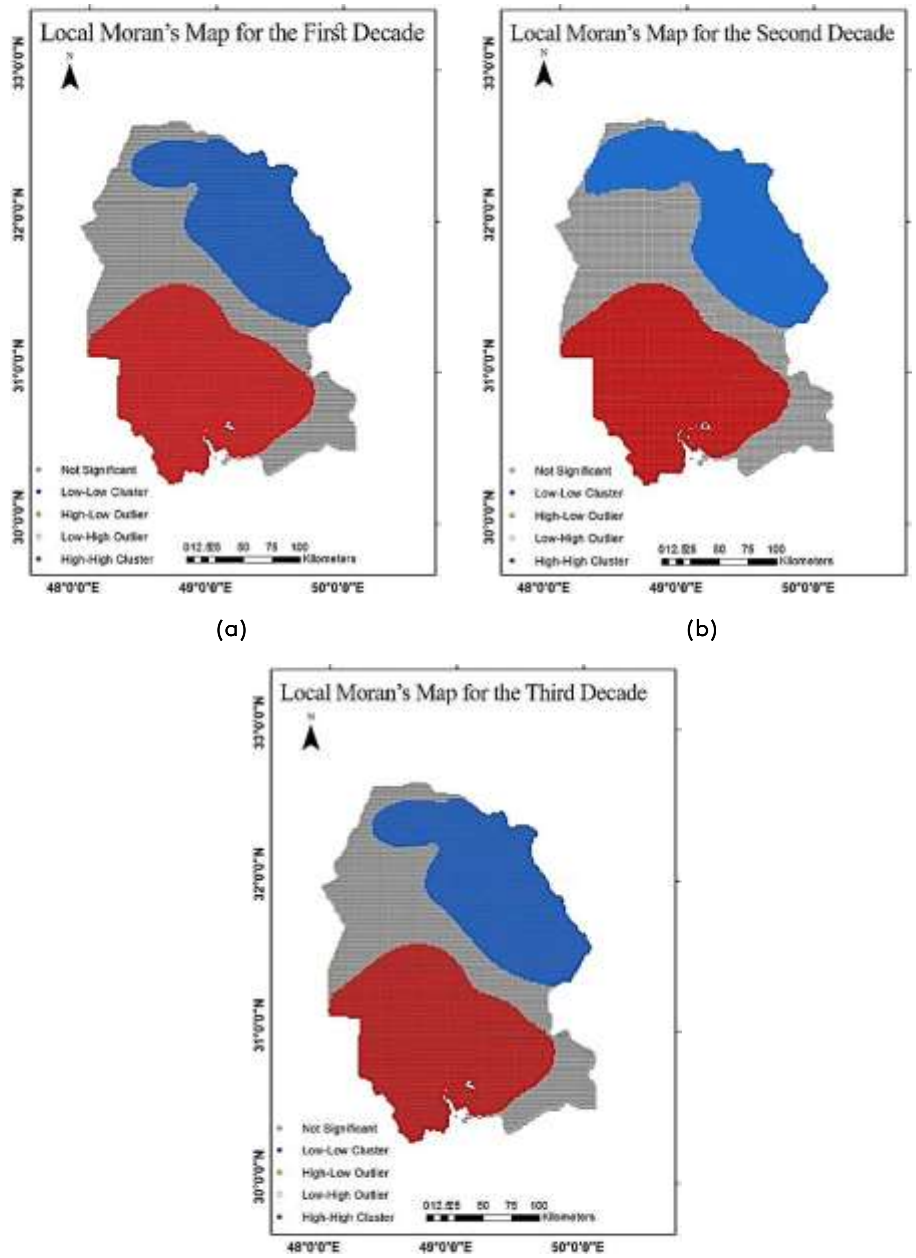

(a) (b)

(c)

Fig. 12. The Local Moran map for droughts in the studied decades based on the SPEI. a) First, b) Second, c) Third decades.

5. Conclusions

Although the geostatistical results of both the SPI and SPEI in Getis-Ord G* were used to identify drought hot and cold spots, the SPEI displayed a more solid performance in identifying drought hot spots. The hot spot maps obtained from the SPI indicated that in many examined months, most regions were non-significant. Also, there was not a sufficiently significant (Moran's correlation) relationship between these regions, but the hot spots introduced by this statistic matched those from the SPEI. The agreement between the hot spots obtained from SPI and SPEI suggested that the drought hot spots were located in the southern and southwestern regions. It is of note that stations and points in this area were the starting points of drought and dust centers. Points having a 99% confidence level would be more effective in this regard. Also, weighing the 10-year total precipitation map against the drought hot spots, the decadal map revealed that in places where the total 10-year precipitation was below 270 mm, drought hot spots were formed with a 99% confidence level. Hot spot maps were alike in all three decades studied. In all decades, hot spots were located in the southern half of the province, while drought cold spots were in the northern half. The Local Moran drought maps of all three decades were similar. In this respect, in all three decades, high-high drought points were located in the southern and southwestern regions. In contrast, low-low drought points were located in the northern and northeastern regions of Khuzestan. Hence, drought concentration extended from the center to the south during the three decades. Using various drought indices simultaneously and identifying drought clusters and drought hot spots allows achieving better results for drought monitoring. The present study determined the extent of the drought's impact and identified the regions with a high drought risk. Overall, the identified hot spots and strong drought clusters are more likely to suffer from drought. The results of drought indices in this study show that the parts with more drought intensity are identified as hot spots in the spatial statistics section. The reason is that the maximum values of the variable are identified for determining these spots, and then the similarity of those values is examined. Thus, in drought analysis, places with more drought intensity are more likely to form hot spots. According to the maps obtained from spatial statistics of drought in this study, the greatest drought crisis in the southern half of Khuzestan is observed in the Abadan, Ahvaz, Mahshahr, and Omidieh stations and the spots between the stations, in the order of their appearance, and this crisis is still increasing. Based on the obtained results, the Abadan, Ahvaz, Mahshahr, Omidiyeh, and Gotvand stations have a higher risk of drought with the highest number of hot spots. Besides, the identified hot spots, especially those identified with SPEI, are highly useful in identifying the dust centers. According to the Khuzestan Crisis Management in 2019, the Crate Camp and Gheizanieh dust centers are among the primary dust centers in Khuzestan Province. Analyzing the hot spots indicated in this study revealed that these centers are located between the Ahvaz and Mahshahr meteorological stations, i.e., about 45 km from the Mahshahr station and 50 km from the Ahvaz station. In Khuzestan, vast lands are devoted to growing major agricultural products such as paddy rice. However, these regions include the identified hot spots, and the water used for rice cultivation causes a challenge to the potable water supply for the residents. In previous years, paddy cultivation has caused problems in supplying potable water during the summer in the cities and villages of Abadan, Khorramshahr, and Shadegan. The results of this study regarding the identified high-high drought clusters and specified hotspots can help farmers select suitable crops. Khuzestan has a large number of dams used to generate electricity that also store large amounts of rainfall, which is effective in the drought crisis. Since there are a large number of sunny days in the study area, using solar power plants to generate electricity could help with the drought in the southern regions. Furthermore, as torrential rains always occur in this region, flood management is another solution that could effectively reduce the impacts of drought in the region. The present study revealed that the preliminary data from the drought index is the basis for using spatial statistics to study drought. Drought indices are established based on several parameters, each affecting the accuracy of the results differently. Regarding the data limitation in this study, the Hargreaves-Samani (HS) method was used to calculate SPEI. In this context, using satellite imagery to calculate drought can increase the accuracy of identifying hot and cold spots in the study area. For instance, the Normalized Difference Vegetation Index (NDVI) method does not require collecting various parameters to assess agricultural and vegetative drought and only requires the processing of initial images. Regarding the importance of interpolation and its accuracy in the results of spatial statistics analysis, other geostatistical methods such as simple kriging, ordinary kriging, and universal kriging can be used for initial interpolation.

References

[1] Raziei, T., Daneshkar Arasteh, P., Akhtari, R., and Saghafian, B. (2007) Investigation of meteorological droughts in the Sistan and Balouchestan Province, using the standardized precipitation index and markov chain model. *Iran-wWater resources research*. 3 (1), 25–35.

[2] Eslamian, S., Eslamian, F. A. (Eds.). (2017). *Handbook of drought and water scarcity: environmental impacts and analysis of drought and water scarcity*. CRC.

[3] SR, H.A. and D, M. (2016) Water and drought crisis and its impact on urbanization. *3rd Conferences and exhibition of future environmental crisis*.

[4] Bazrafshan, J. and Hejabi, S. (2016) Drought monitoring methods. University of Tehran Press.

[5] Vicente-Serrano, S., López-Moreno, J., Drumond, A., Gimeno, L., Nieto, R., Morán-Tejeda, E., et al. (2011) Effects of warming processes on droughts and water resources in the NW Iberian -Peninsula (1930–2006). *Climate research*. *48*(2), 203–212.

[6] Huang, J., Xue, Y., Sun, S., and Zhang, J. (2015) Spatial and temporal variability of drought during 1960–2012 in Inner Mongolia, north China. *Quaternary international*. *355* 134–144.

[7] Rahman, M.R. and Lateh, H. (2016) Meteorological drought in Bangladesh: assessing, analysing and hazard mapping using SPI, GIS and monthly rainfall data. *Environmental earth sciences*. *75* (12), 1026.

[8] Shin, J.Y., Chen, S., Lee, J.-H., and Kim, T.-W. (2018) Investigation of drought propagation in South Korea using drought index and conditional probability. *Terrestrial, Atmospheric and oceanic sciences*. *29* (2), 231–241.

[9] Modarres, R. and de Paulo Rodrigues da Silva, V. (2007) Rainfall trends in arid and semi-arid regions of Iran. *Journal of arid environments*. *70* (2), 344–355.

[10] Masroor, M., Rehman, S., Sajjad, H., Rahaman, M. H., Sahana, M., Ahmed, R., Singh, R. (2021). Assessing the impact of drought conditions on groundwater potential in Godavari Middle Sub-Basin, India using analytical hierarchy process and random forest machine learning algorithm. *Groundwater for sustainable development*, *13*, 100554.

[11] Masroor, M., Rehman, S., Avtar, R., Sahana, M., Ahmed, R., Sajjad, H. (2020). Exploring climate variability and its impact on drought occurrence: Evidence from Godavari Middle sub-basin, India. *Weather and climate extremes*, *30*, 100277.

[12] Dariane, A. (2003) Reservoir operation during droughts. *International journal of engineering*. *16*(3), 209–216.

[13] Harisuseno, D. (2020) Meteorological drought and its relationship with Southern Oscillation Index (SOI). *Civil engineering journal*. *6*(10), 1864–1875.

[14] Beg, A. A. F., Al-Sulttani, A. H. (2020). Spatial assessment of drought conditions over Iraq using the standardized precipitation index (SPI) and GIS techniques. In E*nvironmental remote sensing and GIS in Iraq* (pp. 447-462). Springer, Cham.

[15] Teixeira-Gandra, C. F. A., da Silva, G. M., Damé, R. D. C. F., Neta, M. C. C. C., Villela, F. A., Méllo, L. B., do Couto, R. S. (2019, October). Evaluation of droughts in the State of Rio Grande do Sul, Brazil, using the standardized precipitation index (SPI) and the Moreno Index (MI). In *international congress on engineering and sustainability in the XXI century* (pp. 125-137). Springer, Cham.

[16] Babaei, F.A. and Alijani, B. (45AD) Spatial analysis of Iran's long-term droughts. Natural geography research. 3 1–12.

[17] Hakimdost, Y., Rastegar, M., Pourzeidi, A., & Hatami, H. (2014). Analysis of the Climate Drought and Its Effects on Spatial Patterns of Location in Rural Settlement (Case study villages in Mazandaran Province). *Journal of geography and environmental hazards*, *3*(3), 61–76.

[18] Jamalizadeh, N. and Zohoorian., P. (2015) Analysis and zoning of droughts in Khuzestan Province. *3rd national conference on sustainable development in geography and planning. Architecture and urban planning, Tehran*.

[19] Mohammadi, M. (2016) Shadegan Wetland Destruction and Environmental Consequences, as well as the effect of this increase on dust

phenomenon in Khuzestan province and neighboring areas. *Third National Conference on Environment, Energy, and Biodiversity.*

[20] Afshar, M. H., Al-Yaari, A., Yilmaz, M. T. (2021). Comparative evaluation of microwave L-Band VOD and optical NDVI for agriculture drought detection over Central Europe. *Remote sensing*, *13*(7), 1251.

[21] Xie, F., Fan, H. (2021). Deriving drought indices from MODIS vegetation indices (NDVI/EVI) and Land Surface Temperature (LST): Is data reconstruction necessary?. *International Journal of applied earth observation and geoinformation*, *101*, 102352.

[22] Gadedjisso-Tossou, A., Adjegan, K.I., and Kablan, A.K.M. (2021) Rainfall and temperature trend analysis by Mann–Kendall test and significance for rainfed cereal yields in Northern Togo. *Sci.* 3 (1), 17.

[23] Fooladi, M., Golmohammadi, M. H., Safavi, H. R., Mirghafari, R., Akbari, H. (2021). Trend analysis of hydrological and water quality variables to detect anthropogenic effects and climate variability on a river basin scale: A case study of Iran. *Journal of hydro-environment research*, *34*, 11–23.

[24] Huang, W., Yang, J., Liu, Y., Yu, E. (2021). Spatiotemporal variations of drought in the arid region of Northwestern China during 1950–2012. *Advances in meteorology*, *2021*.

[25] McKee, T. B., Doesken, N. J., Kleist, J. (1993, January). The relationship of drought frequency and duration to time scales. In *proceedings of the 8th conference on applied climatology* (Vol. 17, No. 22, pp. 179-183).

[26] Alizadeh, A. (1998). Principles of applied hydrology, Astan Quds Razavi. *Emam Reza University, Mashad, Iran (in Persian)*, 14–16.

[27] Hayes, M. and J., M. (1999) Drought indices, In drought happens. Climate impacts specialist, National drought mitigation center. P.8.

[28] Vicente-Serrano, S. M., López-Moreno, J. I., Drumond, A., Gimeno, L., Nieto, R., Morán-Tejeda, E., Zabalza, J. (2011). Effects of warming processes on droughts and water resources in the NW Iberian Peninsula (1930–2006). *Climate research*, *48*(2-3), 203-212.

[29] Wang, B., Shi, W., Miao, Z. (2015). Confidence analysis of standard deviational ellipse and its extension into higher dimensional Euclidean space. *PloS one*, *10*(3), e0118537.

[30] Frank, A., Armenski, T., Gocic, M., Popov, S., Popovic, L., Trajkovic, S. (2017). Influence of mathematical and physical background of drought indices on their complementarity and drought recognition ability. *Atmospheric research*, *194*, 268–280.

[31] Hejazizadeh, Z., Joyzedeh, S. (2010). Introduction to drought and its indexes

[32] Martınez-Cob, A., Tejero-Juste, M. (2004). A wind-based qualitative calibration of the Hargreaves ET0 estimation equation in semiarid regions. *Agricultural water management*, *64*(3), 251–264.

[33] Popova, Z., Kercheva, M., Pereira, L. S. (2006). Validation of the FAO methodology for computing ETo with limited data. Application to South Bulgaria. *Irrigation and drainage: The journal of the International commission on irrigation and drainage*, *55*(2), 201-215.

[34] Balyani, Y. and Doost, H. (2014). Fundamentals of spatial data processing using spatial analysis methods. Azad peyman publications.

[35] Johnston, Kevin, Jay M. Ver Hoef, Konstantin Krivoruchko, and Neil Lucas. *Using ArcGIS geostatistical analyst*. Vol. 380. Redlands: Esri, 2001.

[36] Salimi, S., Balyani, S., Hosseini, S.A., and Momenpour, S.E. (2018) The prediction of spatial and temporal distribution of precipitation regime in Iran: the case of Fars province. *Modeling earth systems and environment*. *4*(2), 565–577.

[37] Martínez, W.A., Melo, C.E., and Melo, O.O. (2017) Median Polish Kriging for space–time analysis of precipitation. *Spatial statistics*. *19*, 1–20.

[38] Joyizadeh, S., Haddadi, S., and Dorraninejad, M. (2017) Spatial statistics (Spatial data analysis).

[39] Mitchel, A. (2009) The esri guide to gis analysis. *ERSI Press.*

[40] Fisher, N., Lewis, T., Embleton, B. (1987). Statistical analysis of spherical data, Cambridge University. *Press, Cambridge*.

[41] Anselin, L. (1988). *Spatial econometrics: methods and models* (Vol. 4). Springer science and business media.

[42] Anselin, L. (2000) Part 2 The Link between GIS and spatial analysis. *Journal of geographical systems*. *2*(1), 11–15.

[43] Anselin, L., Florax, R., Rey, S. J. (Eds.). (2013). *Advances in spatial econometrics: methodology, tools and applications*. Springer science and business media.

[44] Boots, B.N. and Kanaroglou, P.S. (1988) Incorporating the effect of spatial structure in discrete choice models of migration. *Journal of regional science*. *28*(4), 495–510.

[45] Burnham, K. P. (1998). Model selection and multimodel inference. *A practical information-theoretic approach*.

[46] Ord, J.K. and Getis, A. (2010) Local Spatial Autocorrelation Statistics: Distributional Issues and an Application. *Geographical analysis*. *27*(4), 286–306.